

# A new method for identifying weather-induced power system stress using shadow prices

Aleksander Grochowicz<sup>\*1</sup>, Koen van Greevenbroek<sup>\*2</sup>, and Hannah C. Bloomfield<sup>3,4</sup>

<sup>1</sup>Department of Mathematics, University of Oslo, P.O. Box 1053 Blindern, 0316 Oslo, Norway

<sup>2</sup>Department of Computer Science, UiT The Arctic University of Norway, Postboks 6050 Langnes, 9037 Tromsø, Norway

<sup>3</sup>School of Geographical Sciences, University of Bristol, University Road, Clifton, Bristol, United Kingdom, BS8 1SS

<sup>4</sup>School of Engineering, Newcastle University, Newcastle upon Tyne, United Kingdom, NE1 7RU

26th July 2023

**Multi-day resilience challenges in highly renewable power systems are triggered by complex interactions between high load, low renewable availability, electricity transmission and storage dynamics. We show these challenges cannot be rigorously understood from an exclusively power systems, or meteorological, perspective and propose a new method, using electricity shadow prices to identify difficult periods driving system investments. These periods are triggered by wind droughts combined with high load periods of various lengths, which can be detected from weather-dependent inputs. However, purely meteorological approaches fail to identify which events lead to the largest system stress driven by transmission bottlenecks and storage issues. These events do not relate strongly to traditional weather patterns (e.g. weather regimes or the North Atlantic Oscillation). We compile new weather patterns including the impacts of storage and interconnection. Without interdisciplinary studies combining state-of-the-art energy meteorology and modelling, further strive for adequate renewable power systems will be hampered.**

As electricity grids reach ever higher levels of renewable penetration, weather and climate variability become increasingly important for power system operations and planning.<sup>1,2</sup> There has been a large effort to incorporate the impacts of climate variability in power system modelling, and running multi-year simulations is becoming commonplace.<sup>3-8</sup> The energy-meteorology community have characterised the most challenging days for power system operation. These *energy system stress events* are modelled either as peak demand, peak demand–net-renewables (“net load”), or energy shortfall events<sup>9-13</sup> which may include wind droughts,<sup>14</sup> solar droughts and dunkelflauten.

It is becoming common practice to consider times of energy system stress as compound events involving near-surface temperatures, wind speeds (and sometimes irradiance) across large geographic and temporal scales.<sup>15-17</sup> While the basic mechanics of periods with energy scarcity in Europe revolve around extreme near-surface temperatures (for demand) and low near-surface wind speeds (for wind power production), we still lack a detailed understanding of the power system dynamics during these weather-driven extremes, and their exact triggering mechanisms.

In this paper we use PyPSA-Eur,<sup>18,19</sup> an open optimisation model for the European power system, to identify system-defining weather periods for potential net-zero emissions systems. The weather inputs to PyPSA-Eur are converted via the open-source software Atlite<sup>20</sup> from 40 years of ECMWF reanalysis data (ERA5),<sup>21,22</sup> whose gridded weather variables we use to investigate the weather phenomena occurring during times of power system stress. We configure the model with high spatial (181 generation and 90 network nodes<sup>23</sup>) and temporal resolution (1-hourly), making it well-

suited to investigating interactions of the European electricity network with a high share of intermittent renewable sources.<sup>8,24-30</sup> The model is formally a capacity expansion and dispatch optimisation problem, and we solve it for forty individual years (June 1980 – July 2020, preserving winters). We take existing transmission and generation technologies (nuclear and hydropower) into account, but otherwise find the cost-minimal allocation and operation of new renewable generation, storage and transmission technologies (see Methods).

We propose using dual variables (also known as shadow prices) of the optimisation model to filter out and delineate system-defining events. We then classify these events based on the prevailing weather conditions, and determine the main factors leading to continent-wide system stress. Our analysis includes weather-driven load and renewable capacity factors, but also transmission and storage interactions across the European electricity grid.

We find that the design of cost-optimal highly renewable power systems in Europe is almost exclusively driven by difficult weather periods during the winter (November – February). These occur during atmospheric blocking events leading to high heating load and low wind speeds. Our analysis reveals a spectrum of challenges ranging from short events (driven mainly by peak generation capacity) to long events (characterised by persistent energy shortage). Transmission congestion across the continent plays an important role in all system-defining events, highlighting the importance of detailed power systems modelling. The most difficult events are characterised by a combination of high load, persistent low wind speeds, transmission congestion and storage depletion.

<sup>\*</sup>Contributed equally, order decided by coin toss.

## Extended periods drive future energy system design, not extreme days

Traditionally, power grids and generation stock have been designed around fossil fuels which could act as dispatchable generators, especially during peak demand. With increased reliance on variable renewables and balancing via transmission and energy storage, this paradigm breaks down. In particular, the most critical events to system design extend beyond a single hour or day, and identifying such periods no longer depends only on weather data but also power system parameters including storage and transmission.<sup>7,12,31,32</sup>

We propose a re-orientation to studying power system stress through system-defining weather events (see Table 1). In a capacity expansion model we use electricity shadow prices (formally dual variables of energy balance constraints) to reveal which time periods cause additional infrastructure investments. Note, however, that despite this economic interpretation the shadow prices are not comparable to electricity prices in the current European market. Electricity shadow prices determine an hourly total electricity cost (Fig. 1), the yearly sum of these costs being the total annual value of electricity in the model (see Methods). We identify *system-defining events* as time periods with an abnormally high total electricity cost. The total annual value of electricity is closely linked to the total system cost (differing only because of existing infrastructure), which is dominated in this model by investment costs (Fig. S1).

We find that on average across 40 weather years, the single most expensive day accounts for 12.4% of total electricity cost (ranging from 6.6–31.3%), whereas 19 out of the 40 weather years contain a three-week period accruing more than half the total electricity cost (Fig. S2). This heterogeneity of events calls into question the use of representative periods or time slices in energy systems modelling. In particular, continuity of the difficult weather conditions is important. Moreover, we find large variations between different weather years, with the single most expensive week-long period accounting for between 18% and 77% of total respective electricity costs. For context, the total yearly electricity costs range from 216 to 330 billion EUR depending on the weather year.

For the purposes of this study, we filter out system-defining events whose costs exceed 100 billion EUR and last less than two weeks (see Methods for details). These thresholds result in a total of 32 events which all happen between November and February; they are marked in Fig. 1. The events vary in length considerably (between 2 and 13 days), being 7 days long on average.

We find that meteorologically extreme single days<sup>10,11,33</sup> do not reliably identify system-defining events in individual weather years (Fig. S17). While such extreme days almost always lead to high shadow prices, these are not necessarily surrounded by a challenging enough period to have a large impact on system design (e.g. see the events in 1997/98, 2011/12 and 2012/13 from Bloomfield et al.,<sup>11</sup> Figs. S16-17); the same also holds for week-long events (Fig. 1 and Figs. S4-7).

As opposed to methods considering only peak load or

net load, (i.e. peak mismatch between renewable generation and load), using power system optimisation outputs to identify system-defining events takes the complex interactions between storage and transmission into account. Moreover, we need not make assumptions about the availability of storage and transmission in any particular region.

## Power systems stress originates in low renewable availability and spreads across continent

In line with previous research, we find that power system stress occurs in the winter months when temperatures, wind and solar production are low in Europe.<sup>11,32,34</sup> Power systems based on renewables are primarily wind-dependent in the winter, especially in the northern latitudes,<sup>35</sup> making them prone to wind droughts. Using standard cost projections, we see annualised investments of 60.9 bn EUR in wind power (onshore and offshore), 28.4 bn EUR in solar power, 15.2 and 13.3 bn EUR in batteries and hydrogen storage respectively, and 18.4 bn EUR in transmission expansion (mean over 40 individual weather year optimisations — Fig. S1).

We find significant variations in the magnitude and location of stress triggers over Europe across the 32 system-defining events (e.g. Figs. S7-8). Still, all but one identified events are consistently driven by low wind power and high load anomalies (Fig. 2 (a)-(b)) when aggregating over the whole system. Moreover, we find that even though the low wind and high load anomalies during system-defining events are concentrated over certain regions, high shadow prices typically spread to the whole continent (Fig. 3). This is despite a modest maximum allowed transmission investment of 25% compared to the current-day grid value in the model. Only peripheral regions (northern Scandinavia and, to a lesser extent, the Iberian peninsula) have significantly lower shadow prices during some of the events; even then they are much higher than average.

## Transmission and storage requirements interact with energy droughts

While system-defining events can be caused by various meteorological conditions, the most severe events are almost always found to play a large role in the sizing of *all* power system components. Fig. 3 shows a representative example of a week-long system-defining event during December 2007. This period was caused by a high pressure system over central Europe causing a period of prolonged low wind as well as high heating load (Fig. 3 (a)-(b)). The event is identified as difficult by the spiking electricity shadow prices (shown by region in Fig. 3 (c) and over time in (d)).

To discern the roles of transmission and storage during this event, we consider the dual variables of the line capacity constraints and inter-hour storage energy level linking constraints respectively (see Methods for details). While we see in Fig. 2 that the 40-year mean shadow price of congestion  $\mu_{l,t}$  across the network is just below 2 EUR / MW, Fig. 3 (c) shows that  $\mu_{l,t}$  reaches event-average values above 1000 EUR / MW for individual lines. This demonstrates that the event in question is a major factor in driving transmission expansion

Approach	Underlying method	Description
1 Net load	Energy meteorology inputs	Periods of mismatch of load and renewable production.
2 Shadow prices	Capacity expansion	Periods that are defining for system design.
3 Load shedding	Dispatch optimisation	Periods of failure to meet demand.

Table 1: An overview over the three approaches we compare in this study. Approach 1 is commonly used in the literature. We introduce Approach 2 in this study (also see Methods) and validate it with Approach 3 (see Methods).

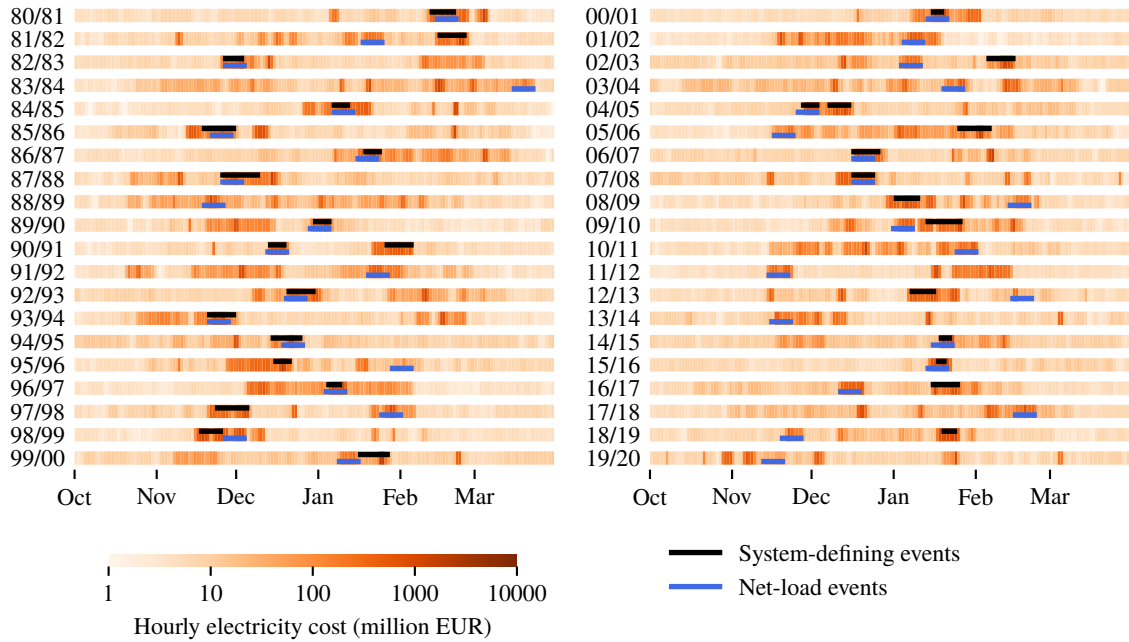


Figure 1: An overview of all identified system-defining events in the context of daily system cost. Additionally the week with the highest net load for each year is marked (Approach 1 in Table 1). Only winter months are shown as shadow prices are consistently low during the summer. All costs are in 2013 EUR, but derive from model shadow prices, not actual market prices.

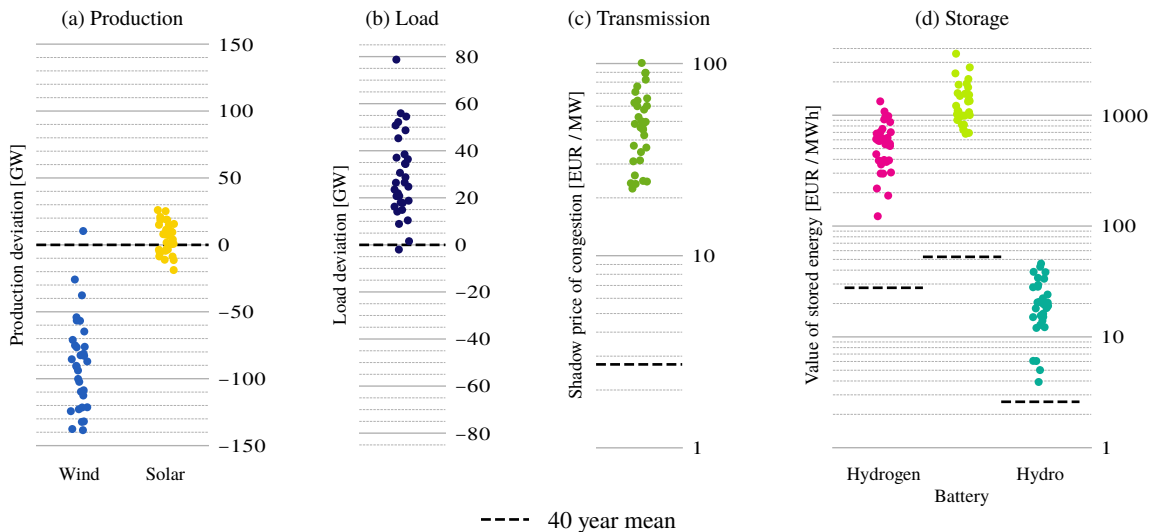


Figure 2: A summary of key metrics compared to 40-year means. Each dot represents the mean value of the metric in question over one difficult period. From left to right: (a) renewable production deviation from 40-year mean at the time of each event, (b) load deviation from 40-year mean at the time of each event, (c) mean shadow price of transmission congestion during each event, (d) mean value of stored energy for each event. An overview over all events can be found in Table S1.

Example: 2007-12-17 16:00:00 - 2007-12-24 08:00:00

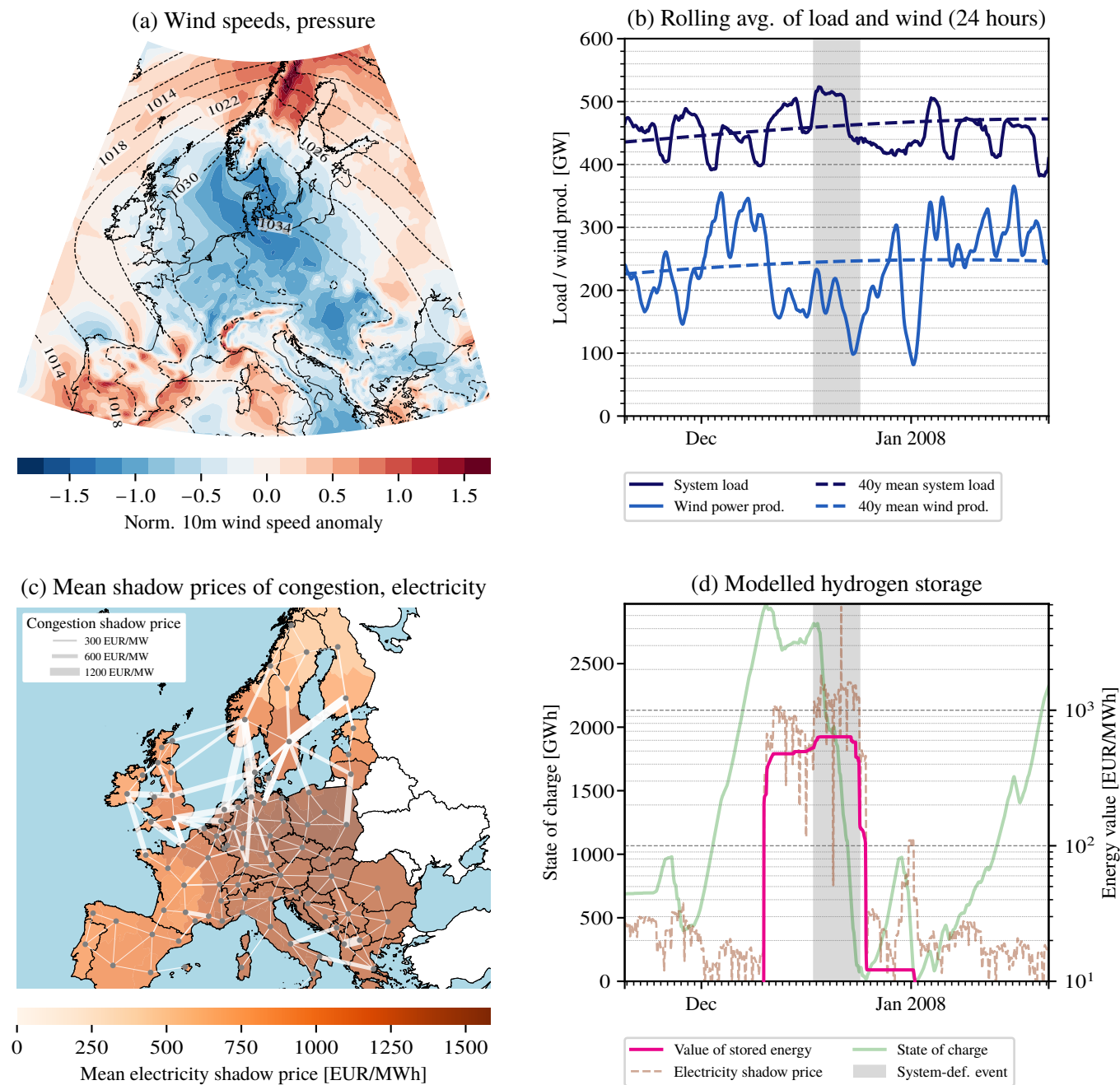


Figure 3: System-defining events are the result of an interplay of low renewable availability, high load, storage constraints and transmission congestion. Inputs in the top row, comparable to a usual meteorological approach (Approach 1). System variables in the bottom row. (a) Average weather in Europe over the example event. Note the wind speed anomalies over the North Sea region and the temperature anomalies in Central Europe in Fig. S9. (b) Time series of wind power production and electricity load around the highlighted event (smoothed with rolling averages of 24 hours). The dashed lines show seasonality deduced from the period 1980–2020. (c) Network map of the European power system with the edge widths showing shadow prices of congestion and the regions shaded with the average electricity price during the event. (d) Time series of electricity prices, value of hydrogen storage (with logarithmic scales), and the hydrogen storage level around the highlighted event (all network averages). All costs are in 2013 EUR.

sion — in fact some 39% of the total annual network congestion rent for the 2007/08 network was gained during the 1-week event depicted in Fig. 3. There is significant congestion between continental Europe on one hand and Scandinavia and the British Isles on the other hand, with significant wind- and hydropower supplied from these regions. The transmission grid is well-connected enough to avoid extreme price spikes in the affected regions.

The value of stored hydrogen energy around the December 2007 system-defining event in Fig. 3 (d) reaches a maximum during the event, but as the marginal electricity prices are higher still, the entire hydrogen storage reserves in the network are discharged. Moreover, this particular system-defining event was preceded by a week-long period of already high prices and high values of stored energy, during which not all hydrogen storage was able to fill up in anticipation of the main event. Other weather years contain meteorologically distinct system-defining periods up to several weeks apart that are nonetheless connected by sustained high values of storage in the interim. This underlines the temporal interdependence of power system dynamics when storage is included, meaning that periods of system stress cannot be studied as isolated events.

## Load shedding provides an alternative method to shadow prices

One commonly used tool to measure power system adequacy is through load shedding (or lost load).<sup>8,36–38</sup> Load shedding can be measured in dispatch optimisations of fixed power system designs, whereas capacity expansion models avoid any load shedding by design.

We expect system-defining events to align with periods of high load shedding; to validate this (see Methods) we calculate for each weather year  $y_i$  the hourly average load shedding in the dispatch optimisations of the power system designs obtained from weather years  $y_j$ ,  $j \in \{1980/81, \dots, 2019/20\}$  operating over year  $y_i$  (a total of 40 dispatch optimisations per weather year). We find that all but one system-defining events overlap with the week-long periods of highest load shedding in the weather year they occurred in.

In any year, system-defining events tend to be those with high load shedding; either method can be used to identify power system stress. Crucially, both shadow prices and load shedding agree on extreme events that are different than those from Approach 1 (Table 1) based only on net load (Figs. S12–S15). This highlights yet again the importance of detailed power systems modelling (also required for computing load shedding) in identifying weather stress events.

Arriving at load shedding data takes an additional step: first obtaining one or several system designs and *then* running them in dispatch mode to reveal load shedding. The latter approach also entails additional assumptions: one has to choose which input scenarios to use for capacity expansion steps and dispatch steps respectively.

## Incorporating transmission and storage constraints challenges the traditional relationship between climate and power systems

Composites of the surface weather conditions observed during each of the 32 events from Approach 2 (Table 1) are shown in Fig. 4 (a)–(b). The events are defined by high pressure systems centred over Central Europe and the North Sea region (where the capacity expansion model mainly builds wind power), resulting in cold temperatures and low wind speeds. This is similar to the synoptic situations<sup>9,10,15</sup> seen using Approach 1.

Within Fig. 4 (a)–(b) multiple surface weather conditions are present. K-means clustering is performed on the normalised hourly near-surface temperature and wind speed fields over the 32 events to isolate key weather patterns of interest (see Methods for details). The four clusters shown in Fig. 4 (c)–(j) all include high pressure centres over parts of Europe and low winds over the North Sea. However, each cluster has very different spatial patterns of surface temperature anomalies, which are not seen in studies neglecting transmission and storage constraints.<sup>10,11</sup> If instead each day is assigned to a more traditional Euro-Atlantic weather regimes framework from Cassou,<sup>39</sup> we see a high frequency of Scandinavian blocking (56%). Generally the pattern correlation between each day’s weather and the assigned cluster is low (Fig. S18) motivating the need for more bespoke approaches to extreme energy days.<sup>40</sup>

When considering seasonal extremes, previous studies have shown strong correlations between the North Atlantic Oscillation (NAO) and national demand and wind power generation.<sup>9,41–43</sup> Winters with a negative NAO index have weaker surface pressure gradients across Europe, leading to colder, stiller conditions and higher seasonal demands. Fig. 5 (a) shows positive correlation between the October–March NAO index and European mean wind capacity factor ( $R^2 = -0.52$ ), with similarly strong negative correlations seen for NAO index and European mean load. Significant correlation is also found when costs of electricity (between October and March) are considered ( $R^2 = -0.42$ ). Winters with a negative NAO index generally exhibit higher costs (Fig. 5 (c)). However, there are times where a high cost can happen in a mild winter (e.g. January 1997 in Fig. S10, which experienced a low-wind-cold-snap driving high system costs. This period was very anomalous compared to the rest of the season).

Fully modelling transmission and storage constraints can lead to a different characterisation of the most challenging winters for power system operation than seen in studies entirely based on meteorological input variables. This is particularly important when considering the sub-seasonal to seasonal prediction of extreme energy events.

## Discussion & Conclusions

In this study we investigate difficult weather events for power systems through an integrated approach combining meteorology with power systems modelling. To improve resilience against weather extremes, we show that it is not enough to look at meteorological variables alone (Approach

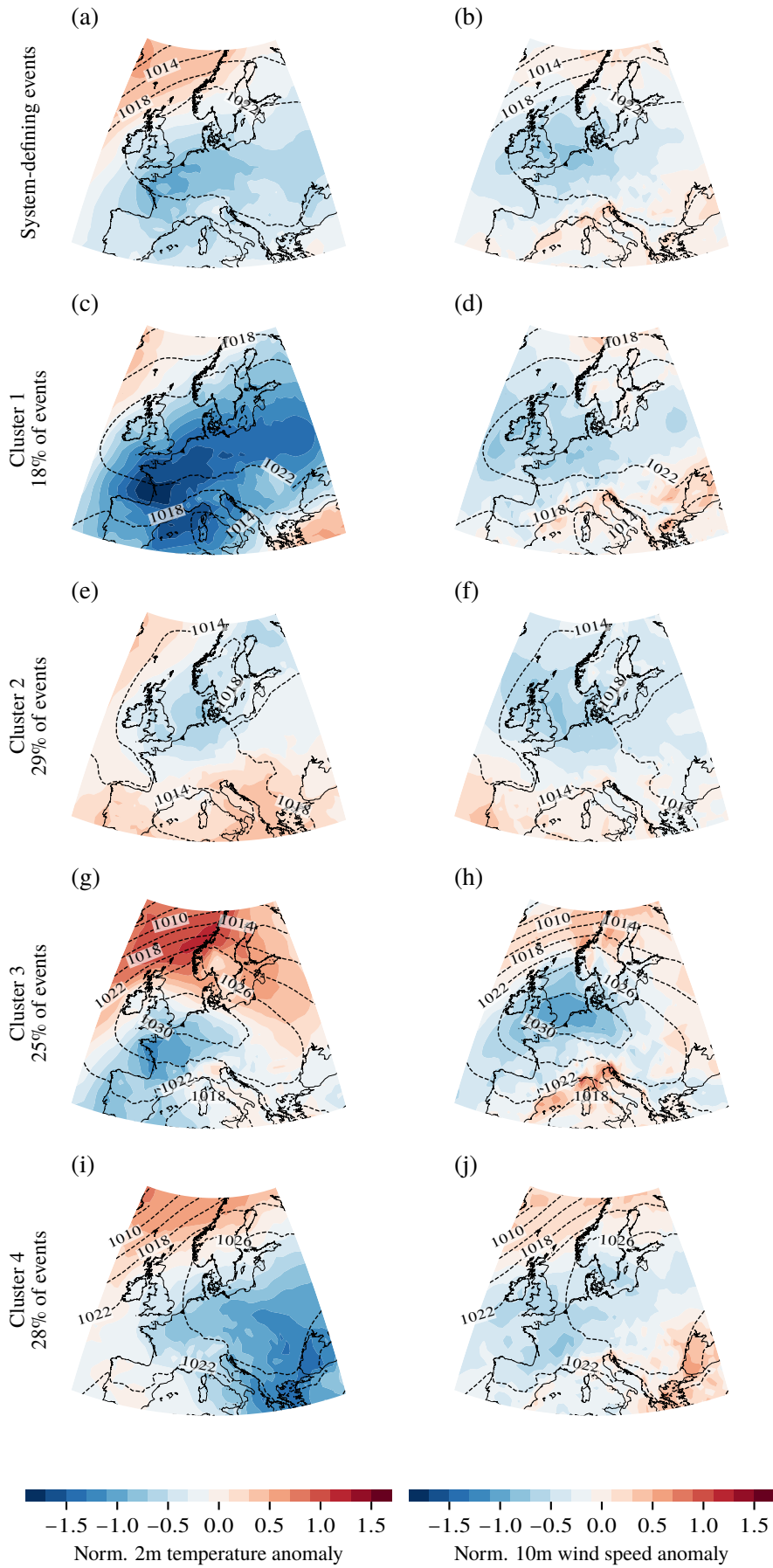


Figure 4: Meteorological conditions during system-defining events (a)–(b). For all 32 events, (c)–(j) are the four extracted clusters of events.

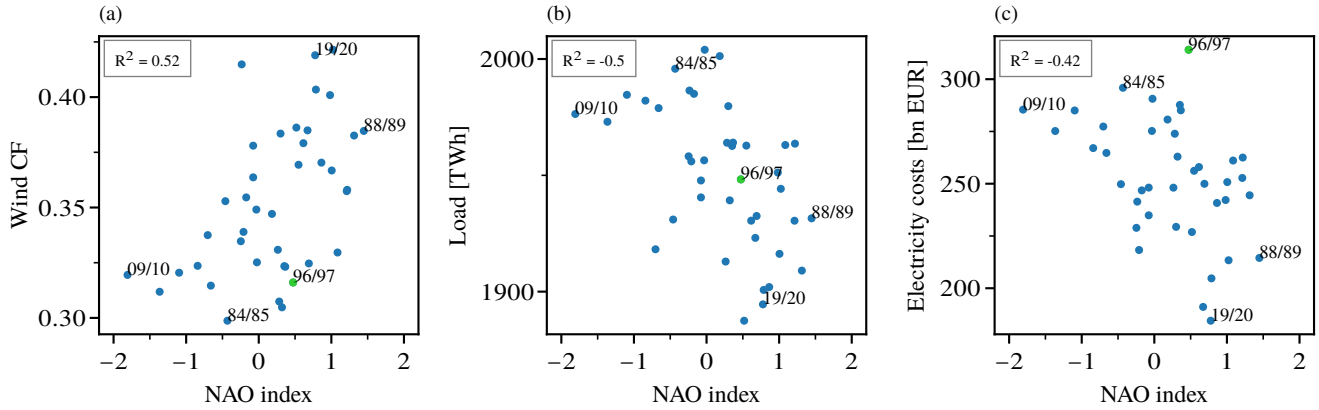


Figure 5: The relationship between October - March mean North Atlantic Oscillation (NAO) index and October - March (a) European mean onshore wind capacity factor, (b) total European net load, and (c) total costs of electricity (all between October and March). The year with the highest costs accrued between October and March (1996/97) is marked with green in (a)-(c).  $R^2$  values show the Pearson correlation coefficient between variables. Similar results are seen for individual countries (not shown).

1), but we also need to include a detailed representation of future, to-be-designed energy systems (Approaches 2 and 3). We propose identifying system-defining weather periods as those being the main drivers of investments; such periods are defined by high electricity shadow prices in a power systems model. As this approach builds directly on modelling outputs, it is free of assumptions on specific characteristics of extreme events.

We find that risk factors like persistent low temperatures and low wind align well with previous literature,<sup>13,14,44</sup> however, conventional meteorological analysis does not reliably identify the most severe difficult periods for future power systems. In particular, challenging periods for the integrated European network vary in duration and are characterised by transmission and storage interactions over time, not only extreme weather. We see that isolated regional studies are not good enough, as the vast majority of the continent experiences uniformly high shadow prices during all system-defining events. To reliably predict future energy system stress events traditional meteorological classifications<sup>10,39,44</sup> are not enough, and more detailed knowledge on surface weather impacts on power systems is needed.

Since our approach is based on single-year optimisations resulting in different system designs for different weather years, electricity shadow prices and thus severity of events are not directly comparable across weather years. This limitation can be addressed by using load shedding (Approach 3 in Table 1) instead of electricity shadow prices to identify extreme events. However, our validation shows that the load shedding and shadow price approaches agree on the most severe events in each individual weather. Computing load shedding is also more computationally expensive and involves more assumptions, requiring a two-step process.

Restricting our analysis to events shorter than two weeks, we capture significant fractions of total electricity cost, but do not capture the full chain of cascading compound events. A complete understanding of how seasonal weather relates to total annual system cost (beyond the partial correlation with the NAO index) is still elusive. Perfect foresight also limits

the ability of our model to react realistically to multi-week or longer events.

An interesting and possible extension of this study would be the inclusion of sector coupling: electrification of heating could strengthen the impacts of heating load and the inclusion of more sectors could lead to different dynamics than in the power sector alone. Still, low wind generation will be key in years to come due to higher penetration of renewable technologies. With ever-improving climate models, these methods could be applied to climate model projections, as system insights based on weather from the 1980s might not necessarily be transferable to mid-century systems under climate change.

The question of pinning down what makes certain weather years difficult (in terms of system costs) remains complicated; the main part of investments throughout the years is driven by a few short-lived and severe events. Our classification can help meteorologists and system operators to develop early warning systems and resilience strategies for these events. It is worth remembering that current systems usually struggle with high load, but that these risks and coping mechanisms will shift towards supply issues when renewable production dominates.

Our flexible approach can be applied to other contexts beyond this European case study and shows that rigid assumption-based analyses within one discipline do not suffice for challenges the world is facing. Our approach exploits inherent information from existing models and unites perspectives from linear optimisation, energy modelling, and meteorology to enhance the understanding on how more resilient future energy systems can be planned. Without interdisciplinary studies with state-of-the-art power system models and meteorological data, progress in researching and implementing renewable energy systems cannot be made.

## Methods

In the spirit of Craig et al.<sup>2</sup> we apply a transdisciplinary approach to identifying challenging weather for power systems. First, we

use outputs from a power system optimisation model to filter out system-defining events that drive investment in additional capacities. For these time periods, we cluster the meteorological conditions into groups such that we can identify weather patterns that drive weather stress events. Then we analyse the effects in the power system (model) during these time periods to determine which components lead to difficulties and are under stress.

## Modelling setup

We represent the European power system by using the open-source energy system optimisation model (ESOM) PyPSA-Eur ([github.com/PyPSA/PyPSA-Eur](https://github.com/PyPSA/PyPSA-Eur))<sup>45</sup> (version 0.6.1) with small modifications. Although capable of a sector-coupled representation of the European energy system, we restrict PyPSA-Eur to the capacity expansion and dispatch optimisation of the power sector. The model performs a partial greenfield optimisation, i.e. with existing transmission network (2019) and capacities of hydropower and nuclear (2022), but without existing renewable capacities. In this formulation, the model minimises the total system costs of the European power system by optimising investment and dispatch of electricity generation, storage, and transmission. Our cost assumptions are based on a modelling horizon of 2030 and we assume a fully decarbonised power system; the available generation technologies are thus nuclear and renewables: hydropower and biomass (non-expandable), solar, onshore and offshore wind power (all expandable). Transmission expansion is limited to 125% of the current level (Fig. 6 in Hörsch & Brown<sup>18</sup>), and electricity can be stored through hydro reservoirs (non-expandable), battery storage and hydrogen storage. For the spatial resolution we follow Fryztacki et al.<sup>23</sup> with 181 generation and 90 network nodes and model the European power system for 40 different weather years (July 1980 – June 2020, preserving winters for each year) with an hourly resolution.

The weather inputs to the power system optimisation model, including wind speeds, solar irradiation, temperatures and runoff, are based on ERA5 reanalysis data<sup>21</sup> and translated to energy variables with the open-source software Atlite.<sup>20</sup> We also use gridded weather variables from ERA5 to investigate the meteorological conditions at times of power system stress.

Many energy system optimisation models (such as PyPSA-Eur) are formulated as a linear program, which means they have a linear objective and linear constraints:

$$\min_{x \in \mathbb{R}^N} c^T \cdot x \text{ s.t. } Ax \leq b, x \geq 0$$

$$A \in \mathbb{R}^{M \times N}, b \in \mathbb{R}^M, c \in \mathbb{R}^N, \text{ for } M, N \in \mathbb{N}.$$

This formulation gives rise to a dual problem

$$\max_{y \in \mathbb{R}^M} b^T \cdot y \text{ s.t. } A^T y \geq c, y \geq 0$$

$$A \in \mathbb{R}^{M \times N}, b \in \mathbb{R}^M, c \in \mathbb{R}^N, \text{ for } M, N \in \mathbb{N}.$$

We are interested in the dual variables that stem from the nodal energy balance constraints for every time step  $t$  and node  $n$ ; equation (12) in Brown et al.<sup>45</sup> These constraints ensure that supply meets a given inelastic electricity demand at each hour and node, and following Brown et al.<sup>45</sup> we denote their respective dual variables  $\lambda_{n,t}$  (also known as marginal or shadow prices). By definition,  $\lambda_{n,t}$  is the rate of change of the objective function, here total system costs, with respect to demand at node  $n$  and time  $t$ . More usefully,  $\lambda_{n,t}$  (given in EUR / MWh) can be interpreted as the marginal electricity price at each node and time step. Letting  $d_{n,t}$  be electricity demand,  $d_{n,t} \cdot \lambda_{n,t}$  is the cost of satisfying electricity load at node  $n$  and hour  $t$ . It follows that  $\sum_{n,t} d_{n,t} \cdot \lambda_{n,t}$  is the total cost of electricity over the entire modelling horizon.

It should be noted that the marginal prices  $\lambda_{n,t}$  typically do not follow the same profile as real electricity market prices; this is due to the inclusion of capacity expansion in our model. This leads  $\lambda_{n,t}$  to not only be driven by marginal operating costs of power plants, as in free electricity markets, but mainly by conditions triggering investments. Thus, the shadow prices  $\lambda_{n,t}$  typically stay very low most of the type, and increase drastically during periods necessitating additional investment in generation, storage and transmission capacity. Nonetheless,  $\sum_{n,t} d_{n,t} \lambda_{n,t} / \sum_{n,t} d_{n,t}$  gives a good indication of the system-average electricity price resulting from the model.

In a simple greenfield capacity expansion model, with no included existing infrastructure, the total cost of electricity  $\sum_{n,t} d_{n,t} \lambda_{n,t}$  (plus the shadow cost of emissions in case of a global emission constraint) is equal to the objective value of the optimisation problem; this following from strong duality for linear programs. Since our model includes existing transmission, hydropower, nuclear and biomass generation infrastructure whose costs are not included in the objective function, the objective value is lower than the total electricity cost. Still,  $\sum_{n,t} d_{n,t}$  is a good indicator for total system cost.

## Identifying system-defining events

In this paper a *system-defining event* is defined as a period where the incurred electricity costs surpass a specified threshold within a limited time frame. We restrict the duration of a system-defining event to last no longer than two weeks, and set the cost threshold to 100 bn EUR resulting in 32 events throughout the 40 weather years. These thresholds result in events that are on average one week long while capturing a significant fraction of total electricity costs; see Fig. S2 for an overview of most costly periods of various lengths for context.

An event starting at  $t_0$  and lasting for  $T$  hours is considered system-defining if

$$\sum_n \sum_{t=t_0}^{t_0+T-1} d_{n,t} \cdot \lambda_{n,t} \geq C \quad (1)$$

for  $C = 100$  bn EUR and  $T \leq 336$  (the number of hours in two weeks).

A priori, many overlapping time periods of the same or different lengths can attain the above thresholds. For example, if the period  $[t_0, t_1]$  is system-defining and strictly shorter than two weeks, then  $[t_0, t_1 + 1]$  is also system-defining. For the purposes of this study, we select a disjoint subset of all system-defining events. In particular, we build up the subset iteratively by going through system-defining events from shorter to longer events (and in decreasing order of total electricity cost for events of the same length), and only adding each event to the selected subset if it does not overlap with previously selected events. This corresponds to imposing a partial order on all system-defining events by defining  $e_1 < e_2$  if and only if  $e_1$  and  $e_2$  overlap and  $e_1$  is shorter than  $e_2$  or, if of the same length, is more expensive; our selected subset consists of the minimal elements of the resulting partially ordered set.

As a final step, we extend the selected events on either side as long as this does not decrease event-average hourly electricity cost. Thus, for the left side of each event, we extend from  $[t_0, t_1]$  to  $[t_0 - 1, t_1]$  as long as

$$\frac{1}{t_1 - t_0} \sum_n \sum_{t=t_0}^{t_1} d_{n,t} \cdot \lambda_{n,t} \leq \frac{1}{t_1 - (t_0 - 1)} \sum_n \sum_{t=t_0-1}^{t_1} d_{n,t} \cdot \lambda_{n,t}. \quad (2)$$

The right side of the events is extended similarly.

## K-means clustering of system-defining events

For each of the 32 system-defining events hourly gridded 2m temperature and 10m wind speeds are taken for the region shown in

Fig. 4 (34N — 72N, 15E — 35E). This gives 5615 hours ( $\sim 233$  days) of data for the k-means clustering analysis. The 2m temperatures and 10m wind speeds are first normalised by their 1980-2021 daily climatologies (by both mean and standard deviation). A similar method as in Cassou<sup>39</sup> is then applied to these datasets. First the data is converted into principal components (the first 14 are kept, explaining 56% of the total variance). These principal components are then grouped into 4 clusters using the k-means algorithm. Four was identified as the optimal number of clusters using the silhouette score as there was no obvious elbow present for the elbow method (not shown). Fig. 4 then shows composites of each cluster which are present for 18, 29, 25, 28 % of the events respectively.

### Traditional meteorological weather regimes approach

Daily October-March 500 hPa geopotential height anomalies from ERA5 are taken over the Euro-Atlantic Region (90W—30E, 20N—80N). Following the classification method of Cassou<sup>39</sup> the first 14 Empirical Orthogonal Functions (EOFs) patterns were computed,<sup>46</sup> which capture 89% of total variance. The associated Principal Component time series (PCs) were used as inputs for the k-means clustering algorithm, with 4 clusters. The four cluster centroids are the positive and negative phases of the North Atlantic Oscillation, the Atlantic Ridge and Scandinavian Blocking (Fig. S18).

The weather regime present during each system-defining event has been calculated, as well as the pattern correlation between the days 500 hPa geopotential height anomaly, and the days cluster centroid as in van der Wiel et al.<sup>10</sup> (Fig. S18).

### Transmission congestion and value of stored energy

For each transmission line  $l$ , the electricity flow  $f_{l,t}$  over that line at time  $t$  is subject to the constraints  $f_{l,t} \geq -F_l$  and  $f_{l,t} \leq F_l$  where  $F_l$  is the capacity of the line in MW and the sign determines the direction of the flow. The dual variables  $\mu_{l,t}^{\text{lower}}$  and  $\mu_{l,t}^{\text{upper}}$  to these constraints are called the shadow prices of congestion. The capacity-weighted sum  $\sum_l (\mu_{l,t}^{\text{lower}} + \mu_{l,t}^{\text{upper}}) F_l$  is the congestion rent of the network, and equal to the surplus gained by the transmission grid at time  $t$ .<sup>47</sup> This way we can judge whether certain periods are determining in the transmission expansion decisions.

Similarly, constraints preserving the state of charge from one hour to the next give rise to dual variables which can be interpreted as the marginal value of stored energy, with each storage unit discharging if and only if its value of stored energy is below the marginal price of electricity at the network node it is connected to.<sup>48,49</sup> It should be noted that these considerations can be a useful indicator for locating crucial regions.

### Validation using load shedding as indicator for difficulty

As a validation of our method to find difficult periods through dual variables, we employ an alternative approach and capture the adequacy of the power system by measuring load shedding in a fixed power system design.

In the context of scenarios for future net-zero-emission power systems, we can first obtain a power system design from a capacity expansion model, and then subject that design to a dispatch optimisation with *different* inputs in order to observe any load shedding. In our case, we might run a capacity expansion model with one weather year  $y_1$ , and perform a dispatch optimisation over a different weather year  $y_2$ . Periods of system stress in weather year  $y_2$  could then be recognised by high load shedding in this dispatch optimisation (Approach 3 in Table 1).

We thus fix system designs  $D_j$ , each obtained by a capacity expansion based on a weather year  $y_j$ ,  $j \in \{1980/81, \dots, 2019/20\}$  (preserving winters from July – June), and optimise the dispatch of  $D_j$  year-by-year with all weather years  $y_i$ ,  $i \in \{1980/81, \dots, 2019/20\}$ . The forty initial optimisations lead to different electricity networks with large discrepancies in total system costs (as in Grochowiec et al.<sup>8</sup>) and are often inadequate for weather conditions that are not represented in the inputs. Keeping the capacities of  $D_j$  fixed, we add an artificial generator at each node  $n$  which can supply electricity at very high variable (and no capital) costs if demand cannot be met any other way. The power supplied by this artificial generator,  $g_{n,t}^j$  can be interpreted as load shedding and quantifies the extent and times during which the system fails to meet demand.

For each weather year  $y_i$ , we compute the average load shedding  $\bar{\ell}_t$  across all 40 system designs  $D_j$  (although  $D_i$  cannot have any load shedding for  $y_i$  by the model formulation), thus obtaining values for each time step between July 1980 and June 2020:

$$\bar{\ell}_t = \frac{1}{40} \sum_j \sum_n g_{n,t}^j, \quad (3)$$

where  $g_{n,t}^j$  is the load shedding at node  $n$  when the system design  $D_j$  is operated at time  $t$ .

One advantage of using load shedding over electricity shadow prices is that latter may suffer from “overshadowing” effects. Since shadow prices indicate events triggering investment, one event might overshadow another in the same weather year if one is slightly more severe than the other but similar otherwise, thus triggering investments (leading to high shadow prices) that render the second event benign. We see limited evidence of this in Fig. S16 (comparing electricity shadow prices and load shedding), but shadow prices and load shedding match well for the most severe events (Figs. S12–15).

### Code and data availability

The code to reproduce the results of the present study, as well as links to the data used, are available at <https://github.com/koen-vg/stressful-weather/tree/v0>. All code is open source (licensed under GPL v3.0 and MIT), and all data used are open (various licenses).

### Acknowledgements

ERA5 reanalysis data<sup>21</sup> were downloaded from the Copernicus Climate Change Service (C3S).<sup>22</sup>

The results contain modified Copernicus Climate Change Service information 2020. Neither the European Commission nor ECMWF is responsible for any use that may be made of the Copernicus information or data it contains.

The computations were partly performed on the Norwegian Research and Education Cloud (NREC), using resources provided by the University of Bergen and the University of Oslo. <http://www.nrec.no/>.

### References

- [1] Bloomfield, H. C. *et al.* The Importance of Weather and Climate to Energy Systems: A Workshop on Next Generation Challenges in Energy–Climate Modeling. *Bulletin of the American Meteorological Society* **102**, E159–E167 (2021).
- [2] Craig, M. T. *et al.* Overcoming the disconnect between energy system and climate modeling. *Joule* **6**, 1405–1417 (2022).

- [3] Pfenninger, S. Dealing with multiple decades of hourly wind and PV time series in energy models: A comparison of methods to reduce time resolution and the planning implications of inter-annual variability. *Applied Energy* **197**, 1–13 (2017).
- [4] Zeyringer, M., Price, J., Fais, B., Li, P.-H. & Sharp, E. Designing low-carbon power systems for Great Britain in 2050 that are robust to the spatiotemporal and inter-annual variability of weather. *Nature Energy* **3**, 395–403 (2018).
- [5] Collins, S., Deane, P., Ó Gallachóir, B., Pfenninger, S. & Staffell, I. Impacts of Inter-annual Wind and Solar Variations on the European Power System. *Joule* **2**, 2076–2090 (2018).
- [6] Schlott, M., Kies, A., Brown, T., Schramm, S. & Greiner, M. The impact of climate change on a cost-optimal highly renewable European electricity network. *Applied Energy* **230**, 1645–1659 (2018).
- [7] Kaspar, F. *et al.* A climatological assessment of balancing effects and shortfall risks of photovoltaics and wind energy in Germany and Europe. In *Advances in Science and Research*, vol. 16, 119–128 (Copernicus GmbH, 2019).
- [8] Grochowicz, A., van Greevenbroek, K., Benth, F. E. & Zeyringer, M. Intersecting near-optimal spaces: European power systems with more resilience to weather variability. *Energy Economics* **118**, 106496 (2023).
- [9] Bloomfield, H. C., Brayshaw, D. J., Shaffrey, L. C., Coker, P. J. & Thornton, H. E. The changing sensitivity of power systems to meteorological drivers: A case study of Great Britain. *Environmental Research Letters* **13**, 054028 (2018).
- [10] van der Wiel, K. *et al.* Meteorological conditions leading to extreme low variable renewable energy production and extreme high energy shortfall. *Renewable and Sustainable Energy Reviews* **111**, 261–275 (2019).
- [11] Bloomfield, H. C., Sitters, C. C. & Drew, D. R. Meteorological Drivers of European Power System Stress. *Journal of Renewable Energy* **2020**, e5481010 (2020).
- [12] Ruhnau, O. & Qvist, S. Storage requirements in a 100% renewable electricity system: Extreme events and inter-annual variability. *Environmental Research Letters* (2022).
- [13] Tedesco, P., Lenkoski, A., Bloomfield, H. C. & Sillmann, J. Gaussian copula modeling of extreme cold and weak-wind events over Europe conditioned on winter weather regimes. *Environmental Research Letters* **18**, 034008 (2023).
- [14] Kay, G. *et al.* Variability in North Sea wind energy and the potential for prolonged winter wind drought. *Atmospheric Science Letters* **24**, e1158 (2023).
- [15] Otero, N., Martius, O., Allen, S., Bloomfield, H. & Schaeffli, B. Characterizing renewable energy compound events across Europe using a logistic regression-based approach. *Meteorological Applications* **29**, e2089 (2022).
- [16] van der Most, L. *et al.* Extreme events in the European renewable power system: Validation of a modeling framework to estimate renewable electricity production and demand from meteorological data. *Renewable and Sustainable Energy Reviews* **170**, 112987 (2022).
- [17] Richardson, D., Pitman, A. & Ridder, N. Climate controls on compound solar and wind droughts in Australia. Preprint, *Climate* (2023).
- [18] Hörsch, J. & Brown, T. The role of spatial scale in joint optimisations of generation and transmission for European highly renewable scenarios. In *2017 14th International Conference on the European Energy Market (EEM)*, 1–7 (IEEE, Dresden, Germany, 2017).
- [19] Schlachtberger, D. P., Brown, T., Schramm, S. & Greiner, M. The benefits of cooperation in a highly renewable European electricity network. *Energy* **134**, 469–481 (2017).
- [20] Hofmann, F., Hampp, J., Neumann, F., Brown, T. & Hörsch, J. Atlite: A Lightweight Python Package for Calculating Renewable Power Potentials and Time Series. *Journal of Open Source Software* **6**, 3294 (2021).
- [21] Hersbach, H. *et al.* ERA5 hourly data on single levels from 1940 to present (2018). URL <https://doi.org/10.24381/cds.adbb2d47>.
- [22] Copernicus Climate Change Service (C3S). ERA5 hourly data on single levels from 1940 to present. URL <https://doi.org/10.24381/cds.adbb2d47>.
- [23] Frysztacki, M. M., Hörsch, J., Hagenmeyer, V. & Brown, T. The strong effect of network resolution on electricity system models with high shares of wind and solar. *Applied Energy* **291**, 116726 (2021).
- [24] Victoria, M., Zhu, K., Brown, T., Andresen, G. B. & Greiner, M. The role of storage technologies throughout the decarbonisation of the sector-coupled European energy system. *Energy Conversion and Management* **201**, 111977 (2019).
- [25] Sasse, J.-P. & Trutnevyte, E. Regional impacts of electricity system transition in Central Europe until 2035. *Nature Communications* **11**, 4972 (2020).
- [26] Schyska, B. U. & Kies, A. How regional differences in cost of capital influence the optimal design of power systems. *Applied Energy* **262**, 114523 (2020).
- [27] Victoria, M., Zhu, K., Brown, T., Andresen, G. B. & Greiner, M. Early decarbonisation of the European energy system pays off. *Nature Communications* **11**, 6223 (2020).
- [28] Brown, T. & Reichenberg, L. Decreasing market value of variable renewables can be avoided by policy action. *Energy Economics* **100**, 105354 (2021).
- [29] Victoria, M., Zeyen, E. & Brown, T. Speed of technological transformations required in Europe to achieve different climate goals. *Joule* **6**, 1066–1086 (2022).
- [30] Neumann, F., Zeyen, E., Victoria, M. & Brown, T. The Potential Role of a Hydrogen Network in Europe (2023). [2207.05816](https://doi.org/10.2207/05816).
- [31] Drücke, J. *et al.* Climatological analysis of solar and wind energy in Germany using the Grosswetterlagen classification. *Renewable Energy* **164**, 1254–1266 (2021).
- [32] Mockert, F., Grams, C. M., Brown, T. & Neumann, F. Meteorological conditions during Dunkelflauten in Germany: Characteristics, the role of weather regimes and impacts on demand (2022). [2212.04870](https://doi.org/10.2212/04870).
- [33] van der Wiel, K. *et al.* The influence of weather regimes on European renewable energy production and demand. *Environmental Research Letters* **14**, 094010 (2019).
- [34] Neumann, F., Zeyen, E., Victoria, M. & Brown, T. Benefits of a Hydrogen Network in Europe. *SSRN Electronic Journal* (2022).
- [35] Dvorak, A. J. & Victoria, M. Key Determinants of Solar Share in Solar- and Wind-Driven Grids. *IEEE Journal of Photovoltaics* **13**, 476–483 (2023).
- [36] Schröder, T. & Kuckshinrichs, W. Value of Lost Load: An Efficient Economic Indicator for Power Supply Security? A Literature Review. *Frontiers in Energy Research* **3** (2015).
- [37] Antonini, E. G., Ruggles, T. H., Farnham, D. J. & Caldeira, K. The quantity-quality transition in the value of expanding wind and solar power generation. *iScience* **25**, 104140 (2022).

- [38] Sundar, S., Craig, M., Payne, A., Brayshaw, D. & Lehner, F. Meteorological Drivers of Resource Adequacy Failures in Current and High Renewable Western U.S. Power Systems (2022).
- [39] Cassou, C. Intraseasonal interaction between the Madden–Julian Oscillation and the North Atlantic Oscillation. *Nature* **455**, 523–527 (2008).
- [40] Bloomfield, H. C. *et al.* Quantifying the sensitivity of European power systems to energy scenarios and climate change projections. *Renewable Energy* **164**, 1062–1075 (2021).
- [41] Ely, C. R., Brayshaw, D. J., Methven, J., Cox, J. & Pearce, O. Implications of the North Atlantic Oscillation for a UK–Norway Renewable power system. *Energy Policy* **62**, 1420–1427 (2013).
- [42] Cradden, L. C., McDermott, F., Zubiate, L., Sweeney, C. & O’Malley, M. A 34-year simulation of wind generation potential for Ireland and the impact of large-scale atmospheric pressure patterns. *Renewable Energy* **106**, 165–176 (2017).
- [43] Thornton, H. E. *et al.* Skilful seasonal prediction of winter gas demand. *Environmental Research Letters* **14**, 024009 (2019).
- [44] Grams, C. M., Beerli, R., Pfenninger, S., Staffell, I. & Wernli, H. Balancing Europe’s wind-power output through spatial deployment informed by weather regimes. *Nature Climate Change* **7**, 557–562 (2017).
- [45] Brown, T., Hörsch, J. & Schlachtberger, D. PyPSA: Python for Power System Analysis. *Journal of Open Research Software* **6**, 4 (2018).
- [46] Dawson, A. Eofs: A Library for EOF Analysis of Meteorological, Oceanographic, and Climate Data **4**, e14 (2016).
- [47] Biggar, D. R. & Hesamzadeh, M. R. (eds.) *The Economics of Electricity Markets* (John Wiley & Sons Ltd, Chichester, United Kingdom, 2014).
- [48] Crampes, C. & Trochet, J.-M. Economics of stationary electricity storage with various charge and discharge durations. *Journal of Energy Storage* **24**, 100746 (2019).
- [49] Williams, O. & Green, R. Electricity storage and market power. *Energy Policy* **164**, 112872 (2022).

## A Inter-annual variability of investment decisions

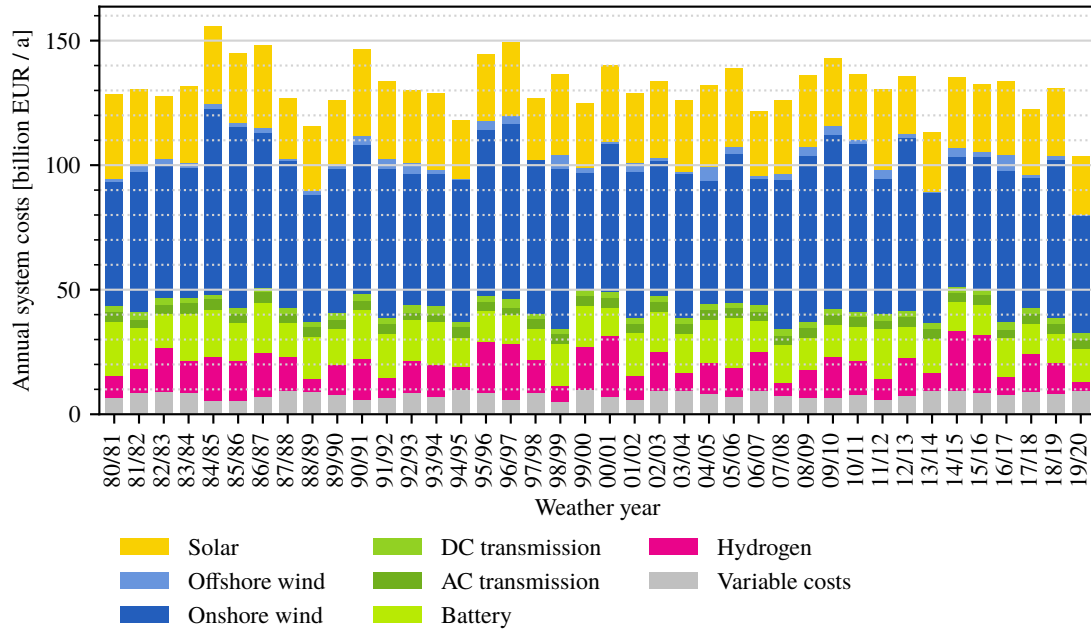


Figure S1: Annualised total system costs of optimal system designs across 40 different weather years after.<sup>8</sup> All costs are in 2013 EUR.

## B Duration and cost of system-defining events

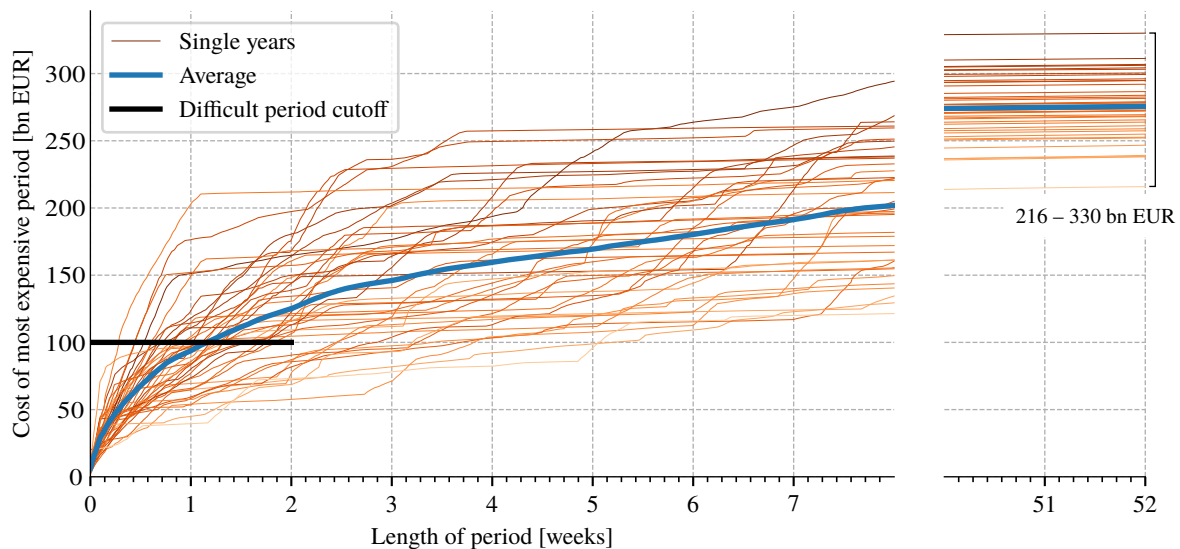


Figure S2: Total electricity costs of most expensive contiguous periods as a function of period length across different weather years. For instance, the vertical slice of the graph at  $x = 1$  week shows that the single most expensive week ranges in cost between about 40 and 200 bn EUR. The thick black line segment shows the cutoff that was used to identify system-defining events: periods of at most 2 weeks having a total electricity cost of at least 100 bn EUR. The weather years without system-defining events correspond to the curves that do not intersect the cutoff line. Note that the cutoff line on this graph cannot be used to identify multiple system-defining events in the same weather year.

### C System-defining events across different years

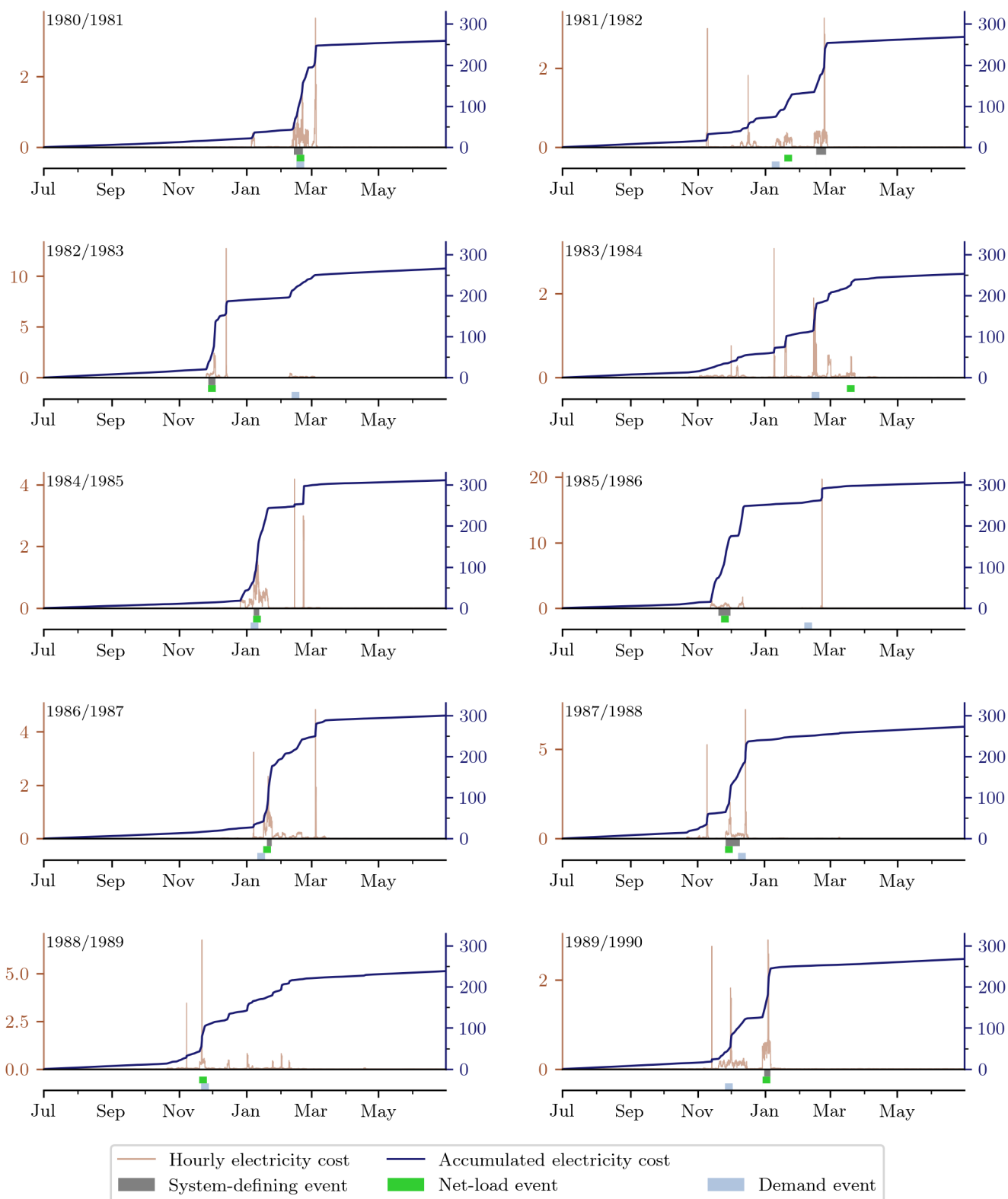


Figure S3: Hourly and accumulated electricity costs across the weather years 1980–1990. System-defining events are marked along with two weather input-based filters: for each year the week with the highest electricity load (“Demand”) and the week with the largest mismatch between electricity load and renewable production (“net load”). All values in bn EUR (2013).

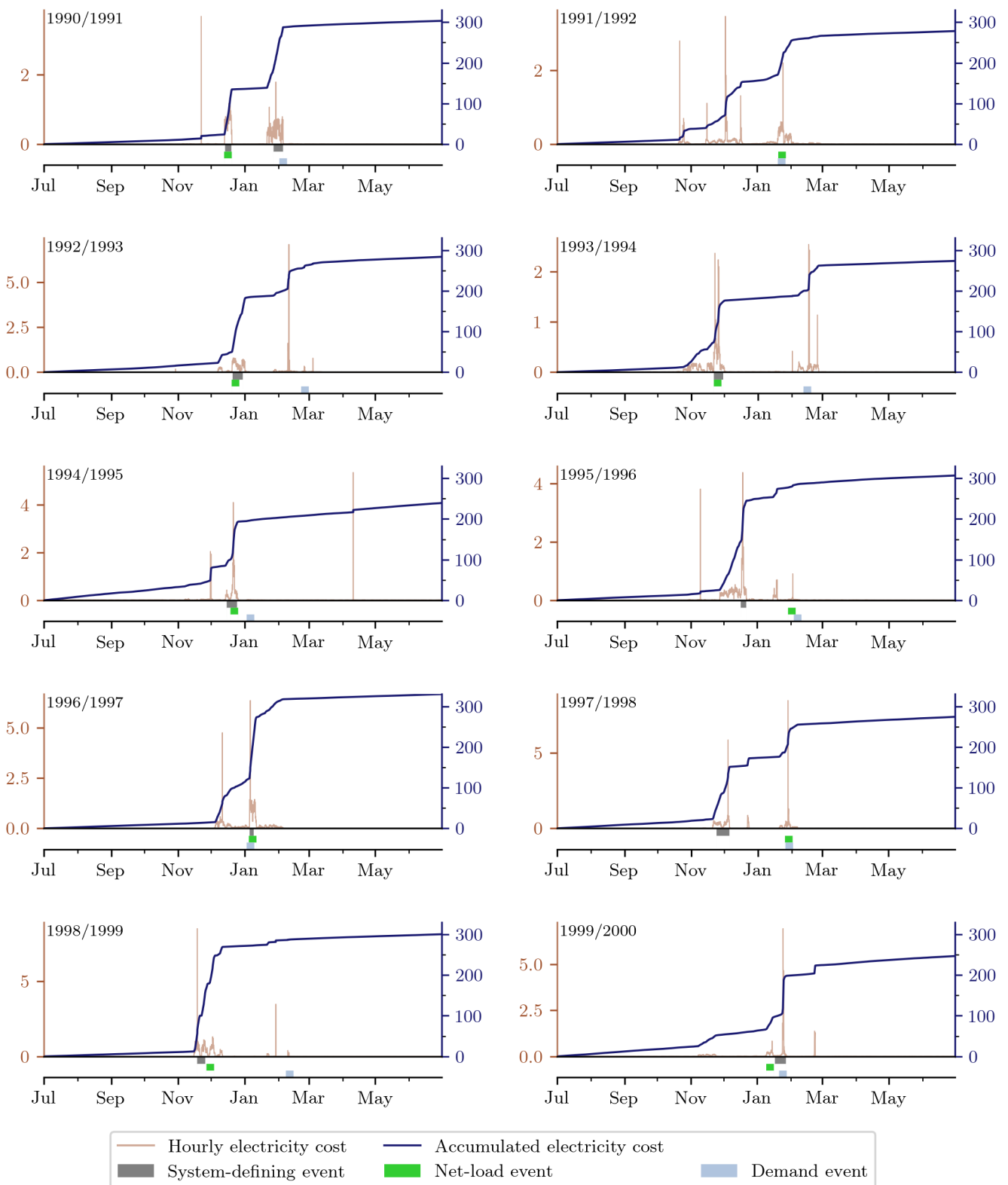


Figure S4: Hourly and accumulated electricity costs across the weather years 1990–2000. System-defining events are marked along with two weather input-based filters: for each year the week with the highest electricity load (“Demand”) and the week with the largest mismatch between electricity load and renewable production (“net load”). All values in bn EUR (2013).

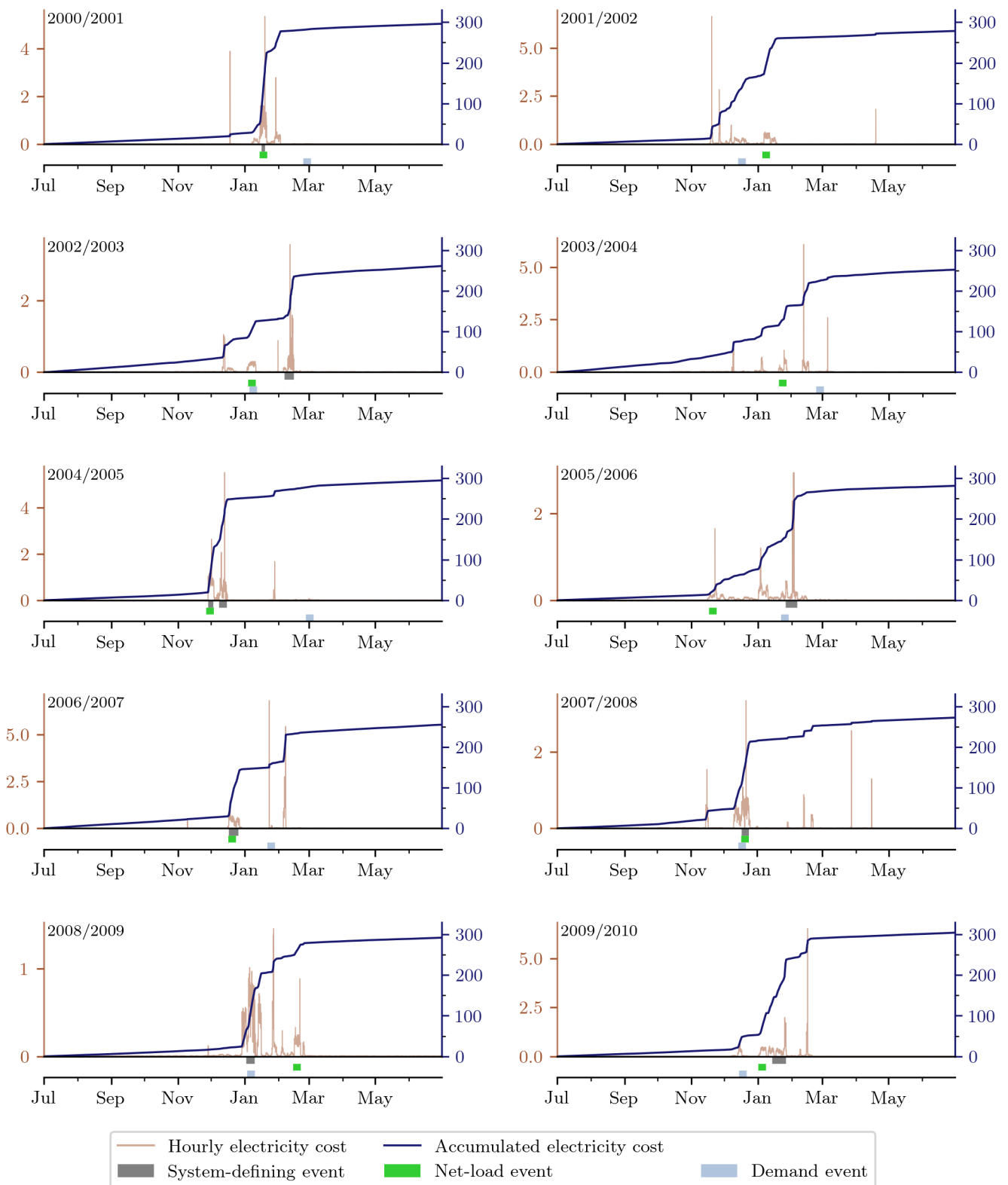


Figure S5: Hourly and accumulated electricity costs across the weather years 2000–2010. System-defining events are marked along with two weather input-based filters: for each year the week with the highest electricity load (“Demand”) and the week with the largest mismatch between electricity load and renewable production (“net load”). All values in bn EUR (2013).

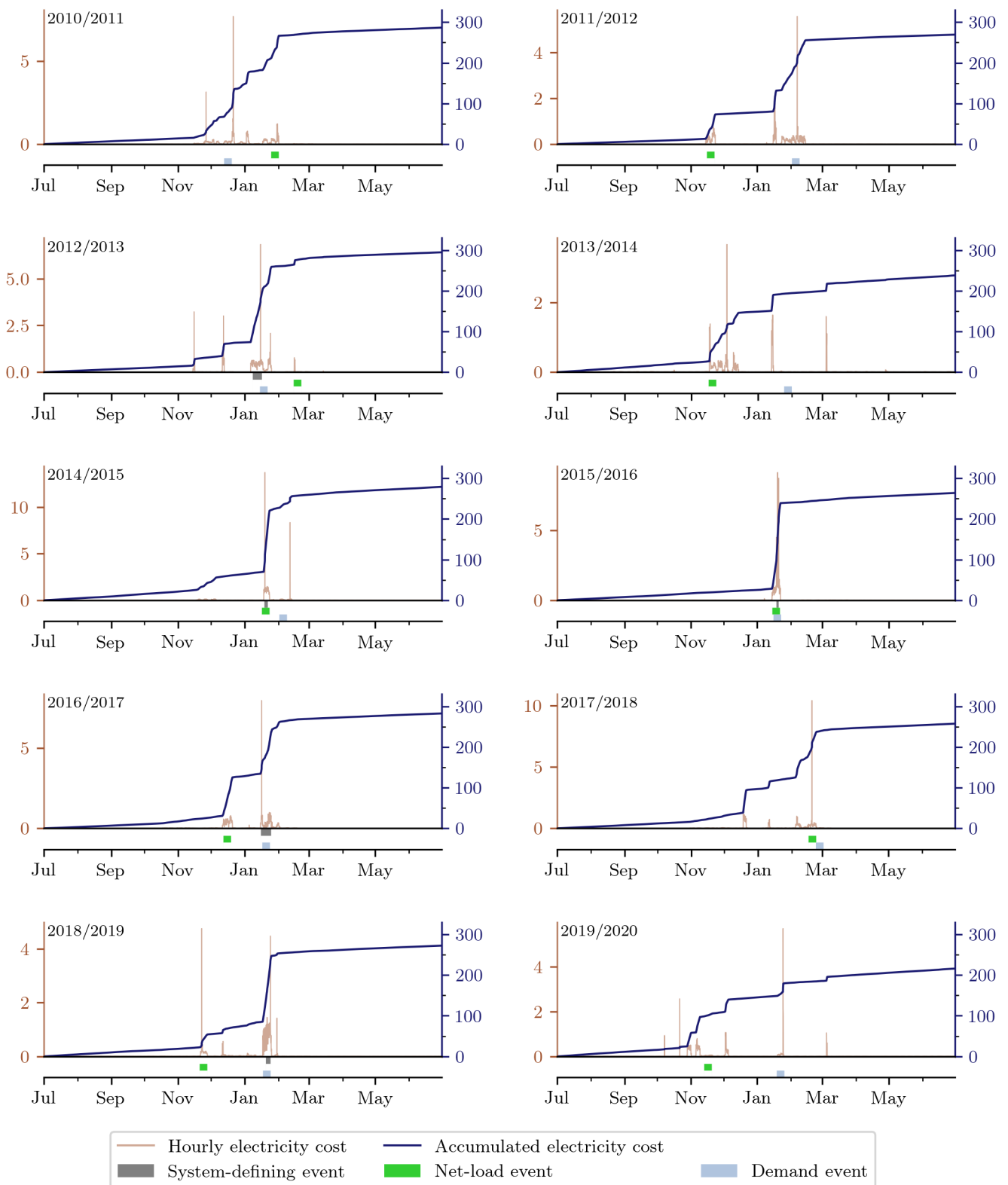


Figure S6: Hourly and accumulated electricity costs across the weather years 2010–2020. System-defining events are marked along with two weather input-based filters: for each year the week with the highest electricity load (“Demand”) and the week with the largest mismatch between electricity load and renewable production (“net load”). All values in bn EUR (2013).

## D Key metrics for the system-defining events

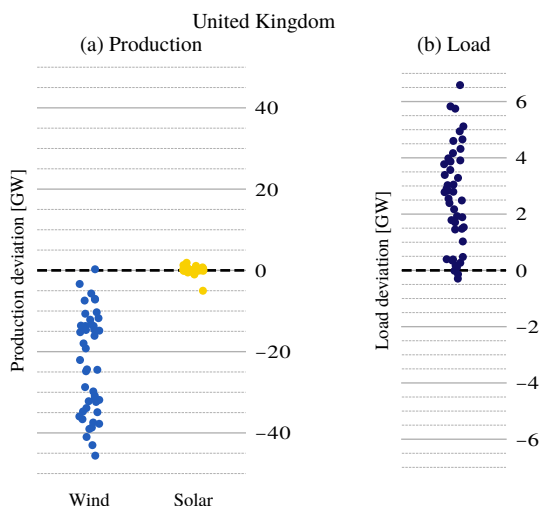


Figure S7: A summary of key metrics for the United Kingdom compared to 40-year means. Each dot represents the mean value of the metric in question over one system-defining event. From left to right: (a) renewable production deviation from 40-year mean at the time of each event, (b) load deviation from 40-year mean at the time of each event.

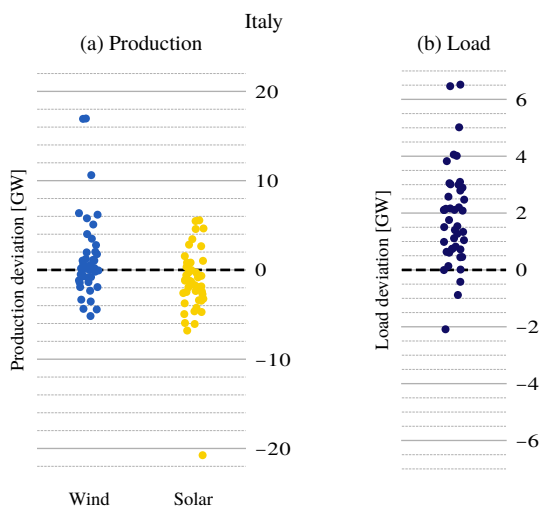


Figure S8: A summary of key metrics for Italy compared to 40-year means. Each dot represents the mean value of the metric in question over one system-defining event. From left to right: (a) renewable production deviation from 40-year mean at the time of each event, (b) load deviation from 40-year mean at the time of each event.

Start	End	Wind anom. [GW]	Solar anom. [GW]	Load anom. [GW]	Transmission [EUR/MW]	Hydrogen [EUR/MWh]	Battery [EUR/MWh]	Hydro [EUR/MWh]
1981-02-13 04:00	1981-02-21 08:00	-93.9	14.8	34.4	22.3	587.2	1102.1	18.2
1982-02-16 12:00	1982-02-25 10:00	-81.4	-3.5	26.5	31.3	359.5	983.0	15.6
1982-11-27 12:00	1982-12-03 23:00	-87.1	-5.1	21.9	36.5	390.1	1329.8	18.1
1985-01-07 16:00	1985-01-12 17:00	-138.4	25.2	78.7	48.5	610.0	1582.3	19.8
1985-11-19 16:00	1985-11-30 15:00	-100.2	-3.1	48.7	23.8	553.5	799.5	6.1
1987-01-19 16:00	1987-01-24 01:00	-137.6	9.6	52.2	49.7	707.4	1885.4	38.6
1987-11-26 15:00	1987-12-09 13:00	-54.1	-4.4	20.7	24.3	297.3	692.5	12.2
1989-12-31 06:00	1990-01-05 21:00	-109.7	18.9	8.9	52.7	545.9	1561.2	20.4
1990-12-14 04:00	1990-12-19 22:00	-132.3	11.3	28.7	48.9	702.5	1493.6	6.1
1991-01-27 16:00	1991-02-05 08:00	-121.3	18.6	36.4	23.6	597.3	1020.7	20.5
1992-12-21 02:00	1992-12-30 10:00	-76.5	7.3	-2.0	34.6	625.2	1003.7	28.3
1993-11-21 16:00	1993-11-30 06:00	-37.7	8.0	50.8	46.5	297.9	992.7	14.0
1994-12-15 16:00	1994-12-25 03:00	-25.9	1.7	10.4	65.9	218.1	822.4	15.2
1995-12-16 20:00	1995-12-21 21:00	-121.5	-8.6	17.8	62.5	391.6	1527.4	24.1
1997-01-05 16:00	1997-01-09 10:00	-122.8	-11.4	45.3	64.1	982.9	2121.7	19.1
1997-11-24 04:00	1997-12-05 23:00	-56.5	-8.7	20.8	45.3	444.8	689.2	15.1
1998-11-18 13:00	1998-11-25 23:00	-56.7	20.9	54.5	46.0	752.4	1083.4	16.2
2000-01-17 06:00	2000-01-27 09:00	10.3	10.5	23.5	37.4	122.6	706.4	5.0
2001-01-16 15:00	2001-01-19 20:00	-124.3	7.8	38.5	76.0	1333.8	2702.0	45.8
2003-02-06 17:00	2003-02-15 07:00	-91.1	9.5	18.8	24.5	304.5	991.8	3.9
2004-11-28 16:00	2004-12-03 09:00	-90.4	-18.8	20.9	60.1	868.4	1785.0	34.1
2004-12-08 16:00	2004-12-15 20:00	-71.0	26.0	14.9	71.2	683.1	1343.6	28.1
2006-01-26 15:00	2006-02-06 06:00	-112.6	8.2	18.0	26.2	188.2	740.4	33.5
2006-12-17 15:00	2006-12-26 09:00	-64.7	4.0	1.6	42.3	527.5	1065.7	18.8
2007-12-17 16:00	2007-12-24 08:00	-75.1	15.6	24.7	82.4	622.4	1383.0	29.5
2009-01-02 15:00	2009-01-10 08:00	-82.9	0.8	34.5	59.9	588.2	1217.3	20.7
2010-01-14 06:00	2010-01-26 21:00	-82.5	-3.6	14.1	31.0	379.0	680.3	12.8
2013-01-08 14:00	2013-01-16 23:00	-102.3	-6.3	16.3	50.0	562.6	905.4	19.5
2015-01-19 06:00	2015-01-22 09:00	-108.7	-11.1	30.6	89.2	1080.6	2386.3	42.9
2016-01-18 16:00	2016-01-20 17:00	-131.9	15.0	55.9	89.6	916.2	3591.0	12.1
2017-01-16 01:00	2017-01-25 10:00	-76.2	18.7	26.4	57.6	394.7	822.4	22.3
2019-01-20 15:00	2019-01-24 21:00	-85.5	0.6	37.1	100.7	970.2	1929.0	38.4

Table S1: Key metrics for all identified system-defining events. The anomalies (to the mean for 1980–2020) for wind power production, solar production, and load are hourly averages in GW, and the values for transmission and the different storage technologies are hourly averages for shadow prices of congestion (in EUR/MW) and value of stored energy (in EUR/MWh).

## E Examples of a system-defining event

2007-12-17 16:00:00 - 2007-12-24 08:00:00

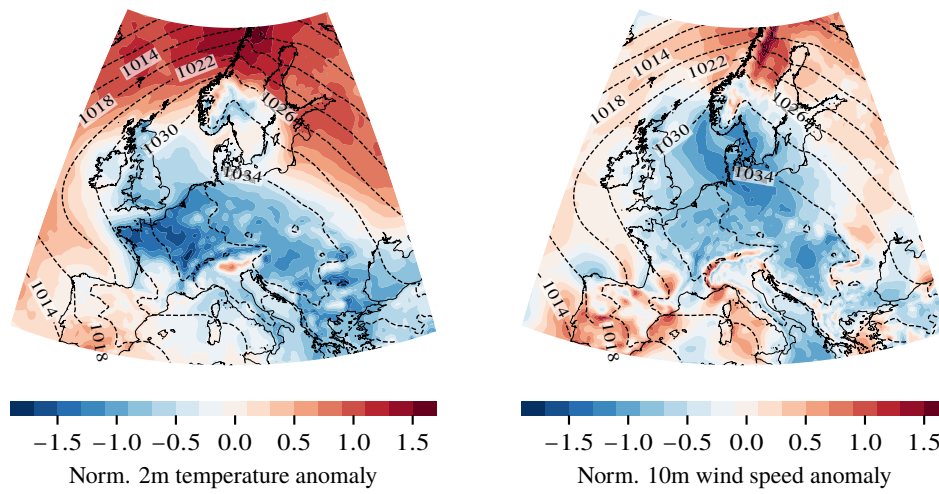


Figure S9: Average weather in Europe over the example event in 2007. Note the temperature anomalies in Central Europe and in particular wind speed anomalies over the North Sea region.

Example: 1997-01-05 16:00:00 - 1997-01-09 10:00:00

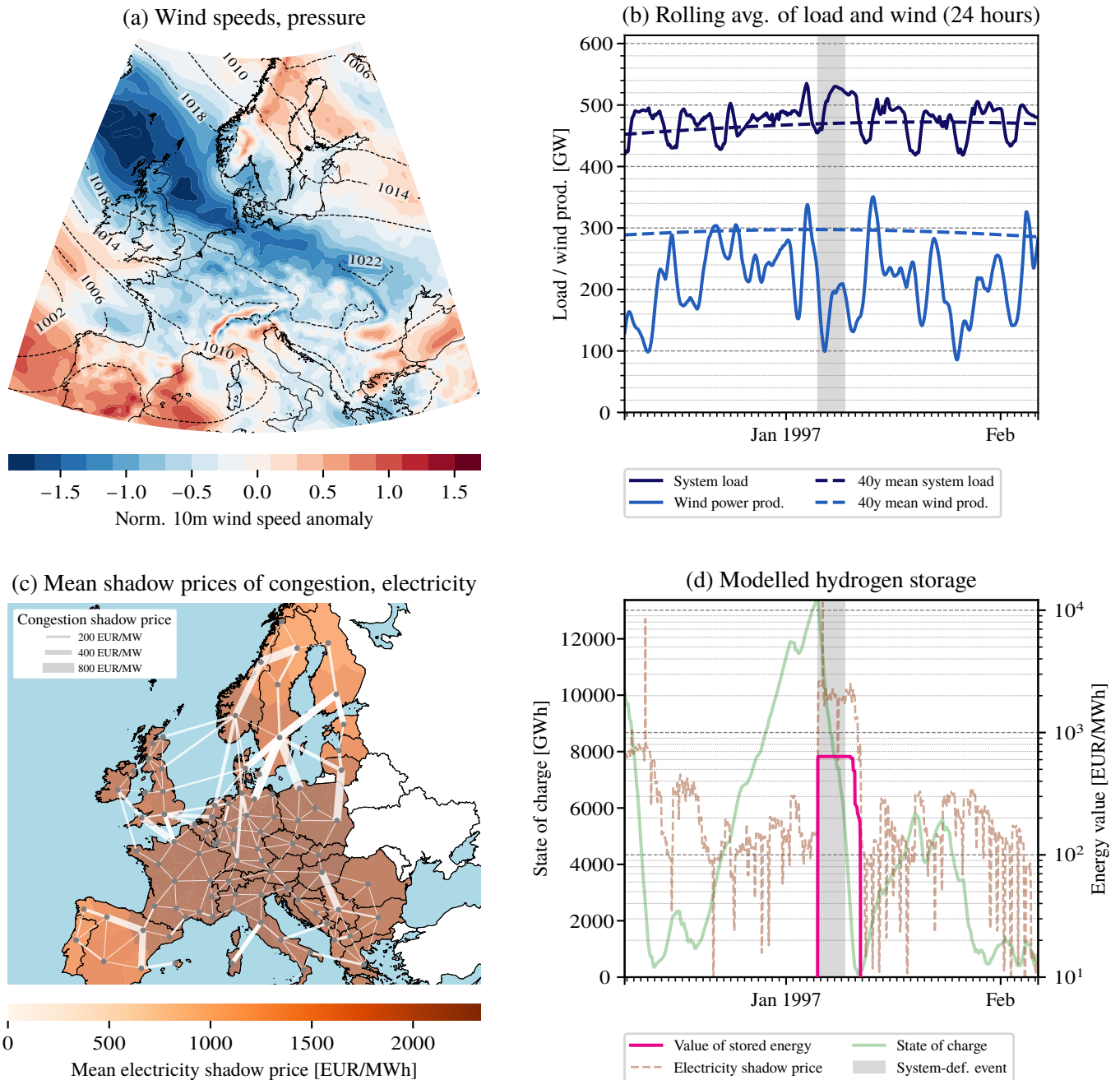


Figure S10: Inputs in the top row, comparable to a usual meteorological approach. System variables in the bottom row. (a) Average weather in Europe over the example event. Note the wind speed anomalies over the North Sea region and the temperature anomalies in Central Europe in Figure S11. (b) Time series of wind power production and electricity load around the highlighted system-defining event (smoothed with rolling averages of 24 hours). The dashed lines show seasonality deduced from the period 1980–2020. (c) Network map of the European power system with the edge widths showing shadow prices of congestion and the regions shaded with the average electricity price during the event. (d) Time series of electricity prices, value of hydrogen storage (with logarithmic scales), and the hydrogen storage level around the highlighted system-defining event.

1997-01-05 16:00:00 - 1997-01-09 10:00:00

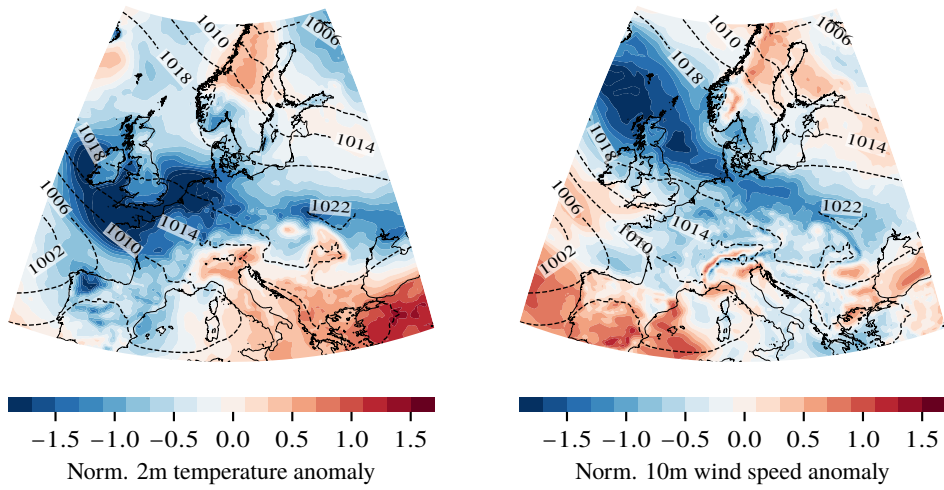


Figure S11: Average weather in Europe over the example event in January 1997.

## F Load shedding provides an alternative method to shadow prices

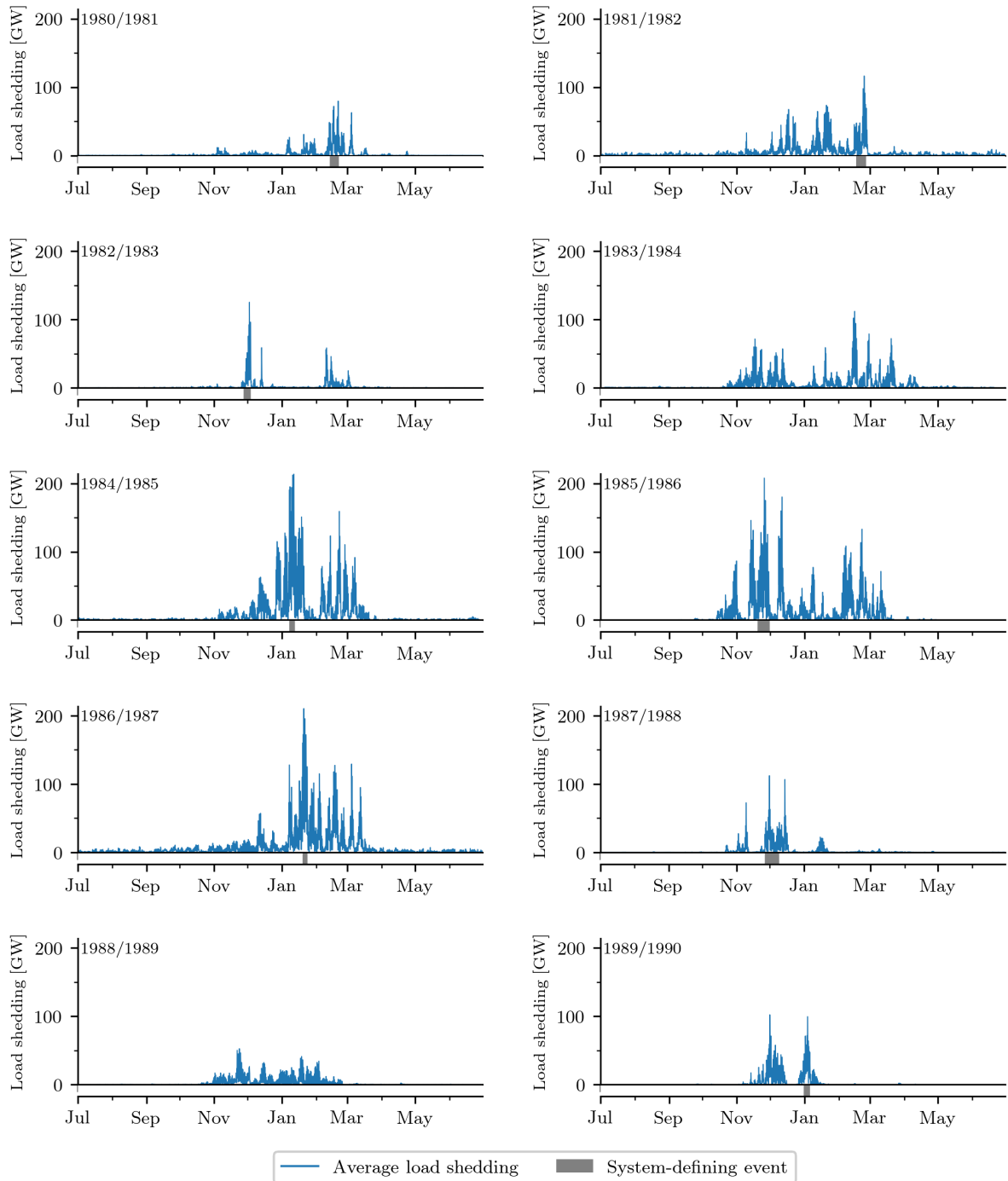


Figure S12: Average load shedding (across all networks) for the weather years 1980–1990. System-defining events are marked.

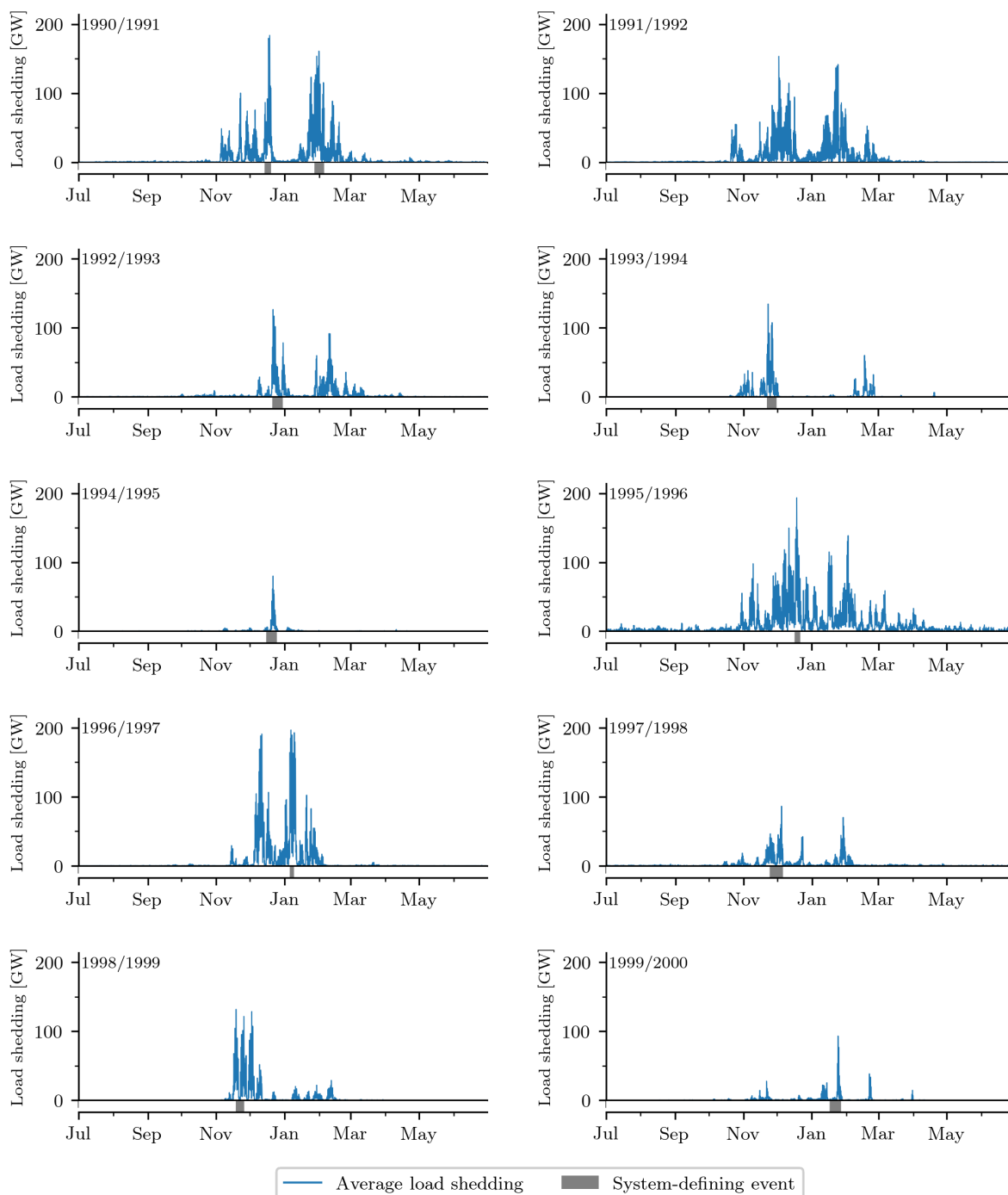


Figure S13: Average load shedding (across all networks) for the weather years 1990–2000. System-defining events are marked.

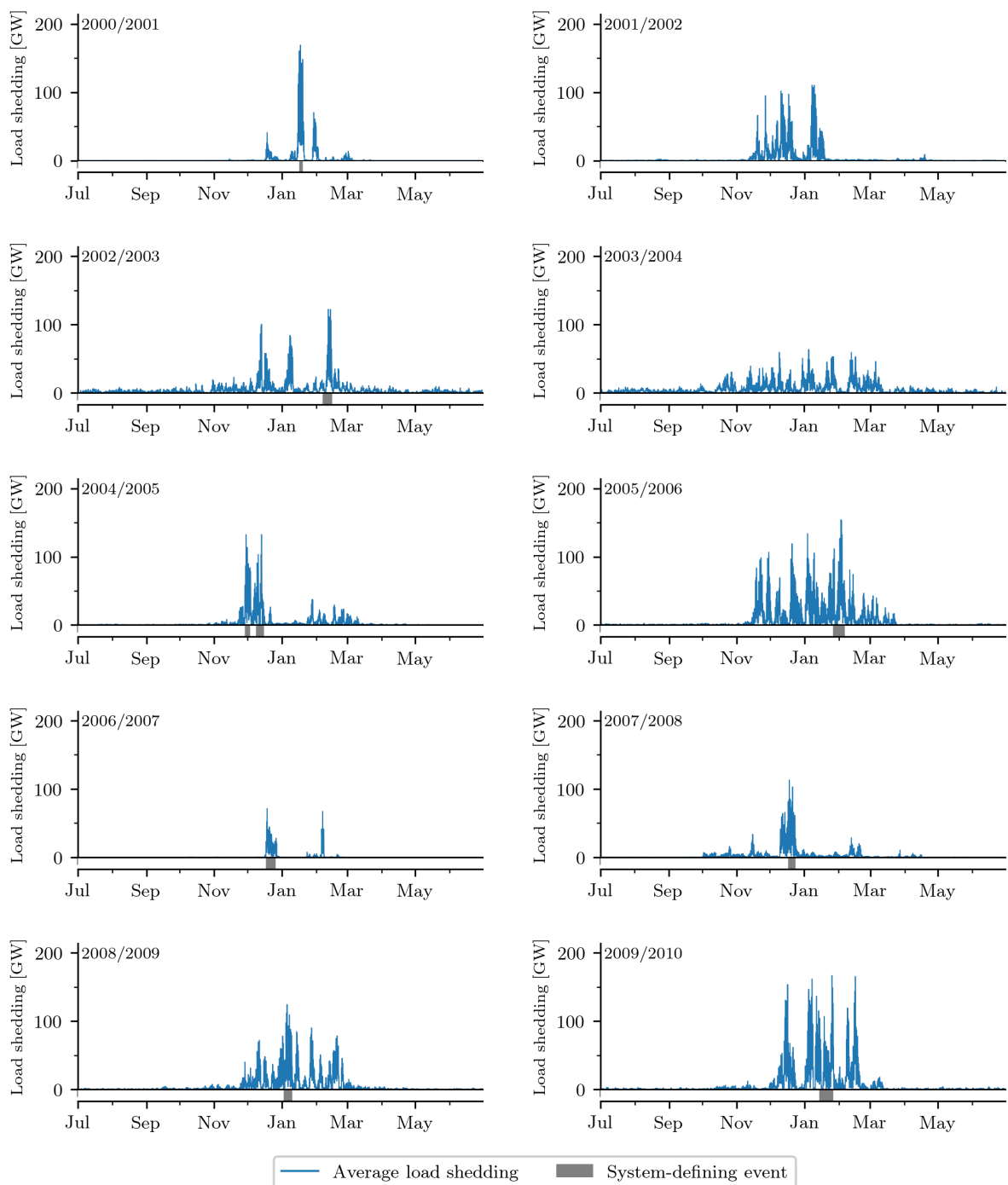


Figure S14: Average load shedding (across all networks) for the weather years 2000–2010. System-defining events are marked.

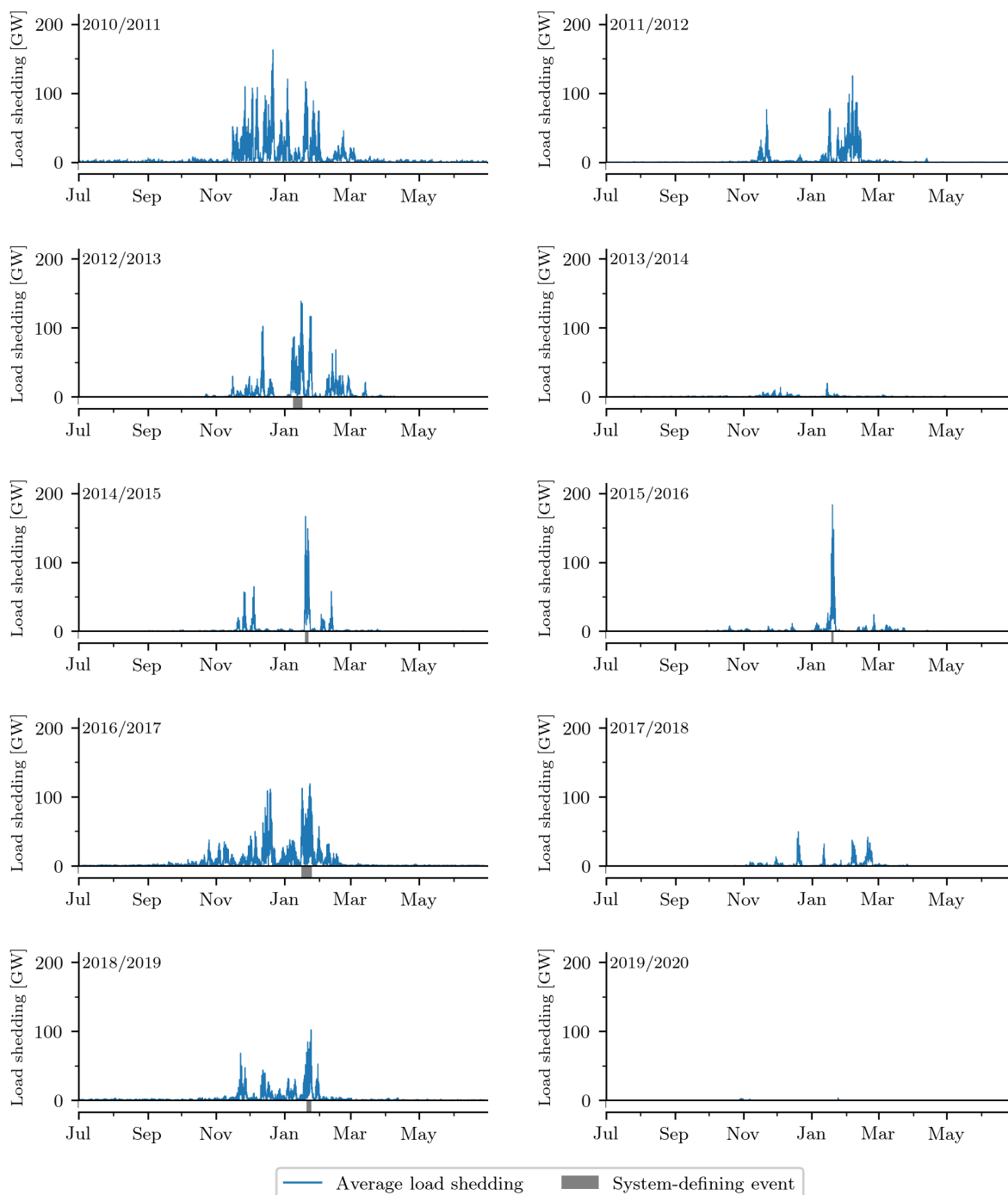


Figure S15: Average load shedding (across all networks) for the weather years 2010–2020. System-defining events are marked.

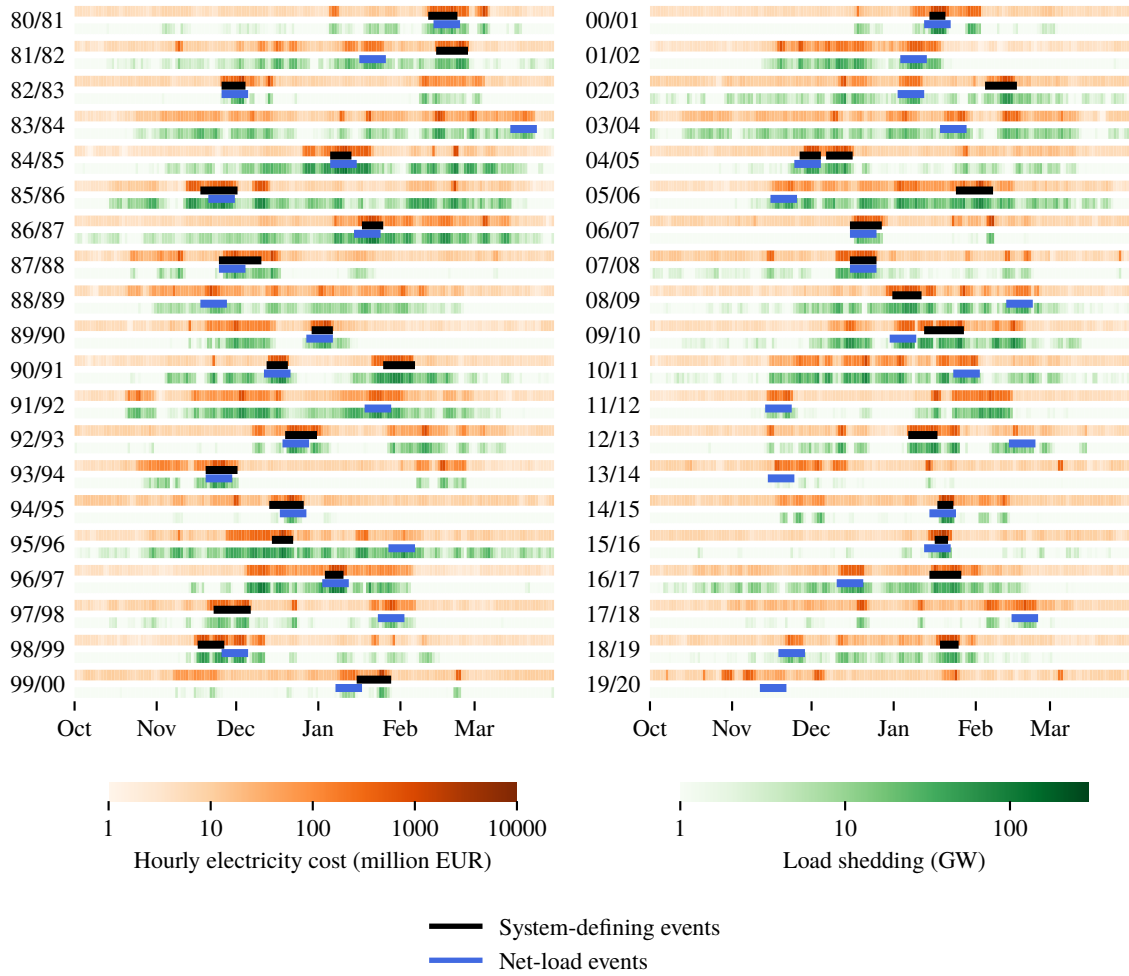


Figure S16: An overview over all identified system-defining events in the context of daily system cost. Apart from the costs we also plot average load shedding (as in Methods). Additionally the week with the highest net load for each year is marked (Approach 1 in Table 1). Only winter months are shown as shadow prices are consistently low during the summer. All costs are in 2013 EUR.

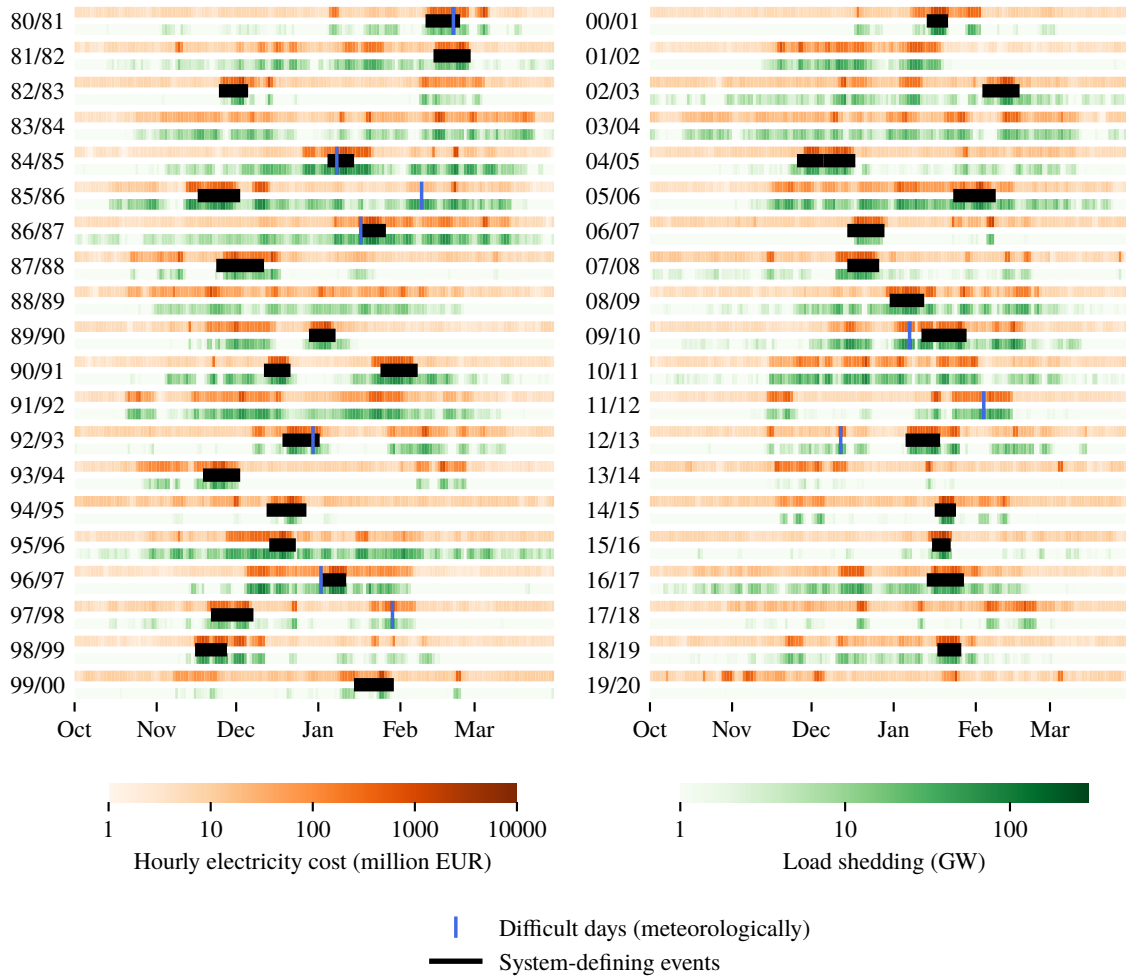


Figure S17: An overview over all identified system-defining events in the context of daily system cost. Apart from the costs we also plot average load shedding (as in Methods). The marked “difficult days” are from.<sup>11</sup> Only winter months are shown as shadow prices are consistently low during the summer. All costs are in 2013 EUR.

## G Euro-Atlantic Weather Regimes during system-defining events

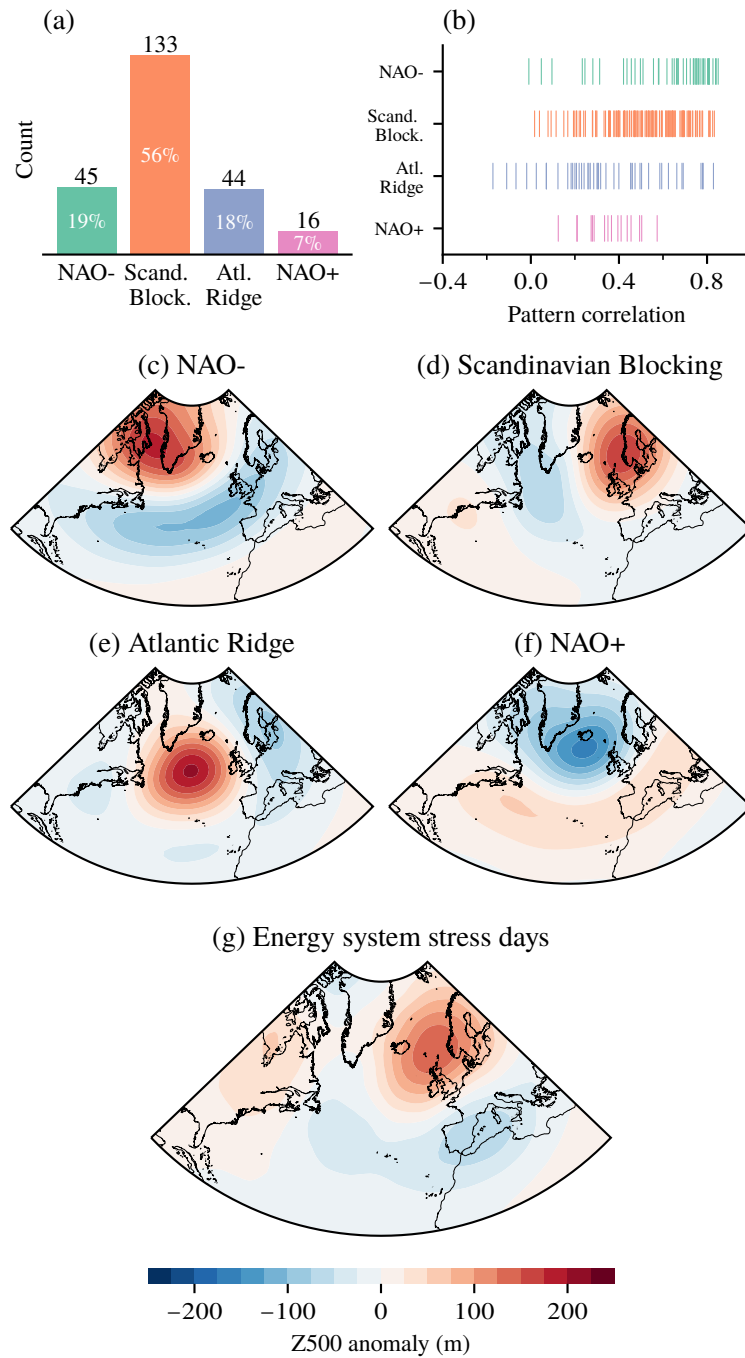


Figure S18: (a) Frequency of occurrence and (b) pattern correlation between the daily 500 hPa geopotential height anomaly from the 32 system-defining events and the four Euro-Atlantic weather regimes as defined in,<sup>39</sup> (c-f) 500 hPa geopotential height (Z500) anomaly composites for the Euro-Atlantic weather regime cluster centroids, (g) Z500 anomaly composite during the 32 system-defining events.